# NASA TECHNICAL MEMORANDUM

NASA TM X- 71964

COPY NO.

NASA TM X-71964

## COMPOSITION SURVEYS OF TEST GAS PRODUCED BY A HYDROGEN-OXYGEN-AIR BURNER

by James M. Eggers

June 1974





NATIONAL AERONAUTICS AND SPACE ADMINISTRATION

LANGLEY RESEARCH CENTER, HAMPTON, VIRGINIA 23665

| 1. Report No. | 2. Government Accession No. | 3. Recipient's Catalog No. |
|---|---|---|
| NASA TM X-71964 | | |

| 4 Title and Subtitle | 5 Report Date |
|---|---|
| COMPOSITION SURVEYS OF TEST GAS PRODUCED BY A HYDROGEN-OXYGEN-AIR BURNER | 6. Performing Organization Code |

| 7. Author(s) | 8. Performing Organization Report No. |
|---|---|
| James M. Eggers | 10. Work Unit No. |

| 9. Performing Organization Name and Address | 11. Contract or Grant No |
|---|---|
| NASA Langley Research Center<br>Hampton, VA 23665 | |

| 12 Sponsoring Agency Name and Address | 13. Type of Report and Period Covered |
|---|---|
| National Aeronautics and Space Administration<br>Washington, D.C. 20564 | Technical Memorandum |
| | 14. Sponsoring Agency Code |

15. Supplementary Notes

Special technical information release, not planned for formal NASA Publication.

16 Abstract

As a result of the need for a uniform hot gas test stream for fuel injector development for hydrogen fueled supersonic combustion ramjet engines, an experimental study of injector configuration effect on exit flow uniformity of a hydrogen-fueled oxygen-replenished combustion burner was made. Measurements used to investigate the burner-nozzle exit profiles were pitot and gas sample measurements. Gas composition and associated temperature profiles were reduced to an acceptable level by burner injector modifications. The effect of the injector modifications was to redistribute the hydrogen fuel, increase the air pressure drop, promote premixing of the oxygen and air, and establish a uniform flow pattern where the oxygen-air mixture comes into contact with the hydrogen fuel. It is believed the most sensitive phenomenon which affected the composition profiles was the uniformity of the air distribution supplied to the combustion chamber. Therefore, designers of combustion burners must recognize the necessity to accept significant air pressure drop to achieve the required uniformity of air distribution.

| 17. Key Words (Suggested by Author(s)) (STAR category underlined) | 18. Distribution Statement |
|---|---|
| Facilities, Research and Support<br>Scramjets<br>Supersonic combustion | |

| 19. Security Classif. (of this report) | 20. Security Classif. (of this page) | 21. No. of Pages | 22. Price* |
|---|---|---|---|
| Unclassified | Unclassified | 47 | $3.25 |

*Available from { The National Technical Information Service, Springfield, Virginia 22151
STIF/NASA Scientific and Technical Information Facility, P.O. Box 33, College Park, MD 20740

# COMPOSITION SURVEYS OF TEST GAS PRODUCED BY A HYDROGEN-OXYGEN-AIR BURNER

James M. Eggers

Langley Research Center

## SUMMARY

As a result of the need for a uniform hot gas test stream for fuel injector development for hydrogen fueled supersonic ramjet combustors, an experimental study of the effect of varying the injector configuration of a hydrogen-fueled oxygen-replenished combustion burner was made. Measurements used to investigate the burner-nozzle exit profiles were pitot pressure and gas samples. By use of the gas sample measurements and helium tracer gas in the oxygen supply, burner-nozzle exit distributions of the three supply gases to the burner, air, oxygen and hydrogen were determined. As complete combustion occurred within the burner, it was possible to estimate local temperature from the local gas composition measurements. Initial unsatisfactory gas composition profiles and associated temperature profiles were reduced to an acceptable level by progressive burner hydrogen-injector modifications. The final modifications consisted of relocating the hydrogen injectors and installing a baffle in the plane of the hydrogen injectors which effected a redistribution of the hydrogen fuel, increased the air pressure drop, promoted premixing of the oxygen and air, and established a uniform flow pattern where the oxygen-air mixture comes into contact with the hydrogen fuel. It is believed the most sensitive phenomenon which affected the composition profiles was the uniformity of the air distribution supplied to the combustion chamber. Therefore, designers of combustion burners must recognize the necessity to accept significant air pressure drop to achieve the required uniformity of air distribution. It was observed that even when severe hydrogen composition and thus large temperature gradients existed, no significant effect on the burner-nozzle pitot pressure was observed. This fact emphasizes the necessity for local gas composition measurements in order to assess the uniformity and thus acceptability of combustion burner performance.

## INTRODUCTION

In order to achieve the capability of designing fuel injectors for supersonic combustion ramjet engines, a suitable uniform hot gas test stream is required. The hot test stream is used to develop and evaluate particular fuel injector configurations, thereby controlling the heat release distribution, and optimizing the combustor design. A hydrogen-fueled, oxygen-replenished burner, as discussed in this report, is one means of providing the hot gas for hydrogen

combustion studies. The burner test gas simulates air to the extent that it contains the proper enthalpy, oxygen volume fraction, and total pressure corresponding to specified flight conditions. The engineering analysis and design calculations for the burner are given in reference 1.

An earlier study reported in reference 2 was conducted to determine the performance of the burner as a function of the burner exit throat area. The burner exit geometry for the referenced study consisted of a choked circular orifice formed by boring a hole in a flange bolted on the burner exit. Various nozzle sizes (throat areas) were simulated by enlarging the orifice in the flange. Reference 2 found a significant temperature profile in the burner exit flow. It was concluded that the measured burner exit temperature profile had a local peak total temperature more than 30 percent greater than the theoretical bulk temperature. The test conditions for which the temperature profile were observed are a burner stagnation pressure of 0.69 $MN/m^2$, a burner total temperature of 1470K and an orifice diameter of 8.89 cm. It was suggested in reference 2 that the temperature profiling could be alleviated by relocating the ring of hydrogen injectors in the burner.

For current combustion studies a Mach 2.70 two-dimensional contoured nozzle replaces the orifice flange used in the study of reference 2. (See figure 1.) The throat area of the two-dimensional nozzle is smaller by a factor of 3.4 than the orifice area corresponding to the measured temperature profile in the referenced study. Preliminary test results with the two-dimensional nozzle indicated a temperature profile problem in the nozzle exit flow similar to that reported in reference 2. For fundamental combustion research studies it is essential that the test gas flow be relatively uniform in pressure, temperature, and composition as skewed profiles do not lend themselves well to analysis or permit ready comparison to other combustion results.

The study reported herein was conducted to investigate the burner-nozzle exit flow for nonuniformities and modify the burner injectors as necessary to produce a relatively uniform test gas flow. Burner stagnation pressures ranged from 2.0 to 2.6 $MN/m^2$ and stagnation temperatures from 2020 K to 2330 K for the present study. Compared to the test conditions of reference 2, the current study was conducted at higher pressures (on the order of 2.9 to 3.8 times higher) and at higher temperature (on the order of 1.4 to 1.6 times higher).

It is noted that the interaction and coupling that occurs in mixing and reacting flows, such as occurs internal to the burner, are not generally amenable to analysis. Therefore, the method of eliminating undesirable profiles at the burner-nozzle exit was accomplished by progressive hardware modifications until satisfactory distributions were achieved.

Unfortunately, test gas temperatures of interest for this study generally exceed the melting point for conventional high temperature thermocouple materials such as Ir-Ir/Rh, particularly when profiling occurs. Thus, thermocouples as used in reference 2 were not applicable to this study. Furthermore, optical devices such as the spectrophotometer, which was used in reference 3 for inferring temperatures and water concentrations, suffer severe limitations in usefulness due to the high noise and vibration level of the test environment.

Therefore, in the study reported herein, uniformity of the burner-nozzle test gas was deduced from instream pitot pressure and gas sample measurements. Results are presented as burner-nozzle exit distributions of hydrogen, oxygen, and air expressed in the unreacted state, and estimated temperature variations deduced from the gas composition.

## SYMBOLS

| | |
|---|---|
| $h$ | burner-nozzle exit height (see figure 2(c)) |
| $P_{t,b}$ | measured burner stagnation pressure |
| $P_{t,2}$ | local pitot pressure |
| $\overline{P}_{t,b}$ | measured burner stagnation pressure divided by the stagnation pressure required to fully expand the burner-nozzle |
| $T_{t,b}$ | theoretical burner stagnation temperature |
| $w$ | burner-nozzle exit width (see figure 2(c)) |
| $y$ | burner-nozzle lateral coordinate (see figure 2(c)) |
| $z$ | burner-nozzle vertical coordinate (see figure 2(c)) |
| $\overline{\alpha}_a$ | local mass fraction of air deduced from the gas sample analysis divided by the bulk (average) mass fraction of air computed from the measured air flow rate to the burner, defined by equation 17 of Appendix A |
| $\overline{\alpha}_o$ | local mass fraction of oxygen deduced from the gas sample analysis divided by the bulk (average) mass fraction of oxygen computed from the measured oxygen flow rate to the burner, defined by equation 18 of Appendix A |
| $\overline{\alpha}_h$ | local mass fraction of hydrogen deduced from the gas sample analysis divided by the bulk (average) mass fraction of hydrogen computed from the measured hydrogen flow rate to the burner, defined by equation 19 of Appendix A |

## APPARATUS AND PROCEDURE

### Combustion Burner

A schematic of the combustion burner is shown in figure 1. The burner

hardware differs from that used in reference 2 in that a two-dimensional Mach 2.70 nozzle replaces the orifice flange used in the referenced study. The nozzle has an exit height of 3.81 cm and a width of 17 cm. The water cooled copper nozzle was designed for uniform parallel flow at the exit and was coated with a 0.13 to 0.25 mm thick thermal protection layer of zirconium oxide. The nozzle, burner, and test hardware are cooled by a high pressure water system. In typical combustion test programs, sufficient oxygen is supplied to the burner such that the resulting test gas simulates air by containing the same volume fraction of oxygen as air. The principal difference between the test gas and air is that due to formation of water from the hydrogen-oxygen reaction, the resulting test gas contains a significant percentage of water. For example, at 2200K the Mach 2.70 test gas contains approximately 36 percent water by volume. For this test program 1 to 2 percent helium by volume was added to the stored oxygen supply as a tracer in order to map the distribution of this oxygen at the burner-nozzle exit. The distinction between pure oxygen and the stored oxygen is not made in the discussion of the data and figures in the main body of this report, as the difference in terms of the final data is insignificant. However, it is necessary to make the distinction in Appendix A which describes the "Gas Sample Data Reduction Procedure."

Various burner injector schemes were tried in order to achieve reasonably uniform burner-nozzle exit profiles. As these injector configurations were progressive in nature and directly associated with the data presented, the injector geometry will be described in the section entitled "Results and Discussion."

Principal measurements consist of oxygen, hydrogen, and air flow rates which are measured by use of sharp-edged orifice plates. Cooling water flow rates, and temperature rise and burner stagnation pressure are other required measurements to define burner operating conditions. These and other associated measurements are recorded by use of a computer controlled magnetic tape data system. Particular pressures, flow rates, and flow rate ratios are computer calculated and immediately displayed post-run to assess whether desired test conditions were achieved.

## Survey Rake

A nine probe pitot-gas-sampling-rake was traversed vertically in steps across the narrow dimension of the nozzle exit flow. A schematic of the survey rake and probe tip detail is shown in figures 2(a) and 2(b), respectively. A water flow rate of 2.2 Kg/sec is used to internally cool the rake. This water then flows through the probe tip units and exhausts rearward providing additional cooling of the external rake surfaces. The coordinate system used to describe the probe's position in the nozzle exit is shown in figure 2(c).

During a typical run time of twelve to fifteen seconds, an automatic rake positioner mechanism permitted a five-point pitot scan (total 45 pitot measurements) or collection of nine gas samples with nine associated pitot pressure measurements. Signals from the transducers that sense the pitot pressure are recorded on an oscillograph for later reduction.

Based upon measurements taken during calibration of the probe travel, the repeatability of the probe positioner is ± 0.025 cm. However, during data acquisition, aerodynamic and heating loads on the rake and probes could increase the uncertainty substantially.

## Gas Sample Collection System

Each of the nine individual probes is connected to a pressure transducer and a 75 cc gas sample cylinder. The exhaust side of each cylinder is in turn connected to a vacuum reservoir system which allows prerun evacuation of the cylinders and aspiration of the flow through the probe-cylinder system. The gas samples are collected by the following procedure: immediately after the rake is inserted into the flow one second is allowed for pitot pressure recording, three seconds for purging of the tubing and sample cylinder, and three seconds for sample collection. Samples collected in this manner are on the order of two or three times the ambient pressure level. The sample collection system is not heated; therefore, water in the gas sample condenses and the gas samples do not contain meaningful water content. The gas sample cylinders are removed from the collection rack and analyzed post-run.

As to whether the gas samples collected are representative of the actual test gas stream is difficult to determine in reactive flows. (For a discussion of the general problem, see reference 4.) Conceptually representative sample collection requires rapid sample cooling to quench the chemical reactions, avoidance of a strong unattached bow shock, and isokinetic (or constant velocity) sampling. These features have been incorporated in the probe tip design shown in figure 2(b) and as much as feasible in the sample collection procedure. Rapid sample cooling is accomplished by conduction from the water-cooled probe and the internal expansion of the probe tip. Shock attachment is encouraged by minimizing the probe tip angle, using a sharp-tipped probe leading edge, internal expansion, and aspiration of the sample during the purge time, and to some degree during sample collection due to the pre-evacuation of the sample cylinders. Isokinetic sampling is probably never actually achieved in turbulent reacting flows as the local velocity varies with time; however, the same features which encourage shock attachment would tend to encourage conditions approaching the isokinetic process.

In the current study, how uniformly a given burner injector arrangement distributes the gases (hydrogen, oxygen, and air) can be evaluated regardless of the sample quenching ability of the probe. However, if further conclusions as to whether the burner operates with complete combustion or if temperature estimates, as discussed in the following section, are derived from the measured gas composition, then the results depend upon the probes quenching ability.

## Gas Sample Analysis

Gas samples were analyzed for oxygen, nitrogen, hydrogen, and helium content by conventional gas-solid chromatography techniques. Details on the concept of gas chromotography will not be discussed herein, as standard text books such as reference 5 are readily available. Briefly, the separation of the

sample into components is accomplished by passing the sample through a column packed with type 13X molecular sieve material. The amount of each gaseous component present is sensed by thermistor detectors and recorded on a strip chart recorder. The recorder output peak heights from the separated gas sample are compared to peak heights for samples of known composition, thus determining the amount of each constituent present. Gas chromatograph parameters are presented in Appendix B.

To define the test gas stream it was necessary to know the local concentrations of helium, hydrogen, oxygen, nitrogen, argon, and water. However, as water condensed in the unheated gas sample lines, the samples collected did not contain meaningful water content. Therefore, the water concentration was computed by the method described in Appendix A, which relies largely upon the use of the helium tracer. The final gas sample results were converted to local concentrations of air, hydrogen, and oxygen (all in the unreacted state). Maldistributions of any of the three supply gases in the burner nozzle exit were therefore related to the associated injector arrangement in the burner.

A further result of the gas sample analysis was an estimate of the local temperature. Assuming representative gas samples are collected, isentropic equilibrium expansion through the burner-nozzle, and complete reaction, the deduced local hydrogen concentration becomes a measure of temperature. For the local gas sample as well as for the overall burner, the ratio of hydrogen to the sum of the air and oxygen defines a temperature computed from equilibrium chemistry (see figure 25 of reference 2) and a heat loss fraction of 13 to 15 percent, which has been found to be representative of the burner for the temperature range of this study. The assumption of complete reaction appears well justified in that no free hydrogen was detected in any of the gas samples collected.

For each gas sample analyzed a check is made on the analysis by summing the volume fraction of all components, including argon which is calculated from the nitrogen percentage. Analysis of several hundred gas samples indicate that summations were 1.0 ± 0.01 for about 90 percent of the samples. As numerous sources of error are possible in analysis ranging from improper injection loop purging to calibration shifts in the instrumentation, the ± 0.01 summation accuracy is considered good. All gas analysis results reported herein satisfy the ± 0.01 summation criteria. Note this criteria does not necessarily detect errors in helium analysis, as the helium volume fractions are low enough that their values do not significantly affect the summation.

## Test Procedure

The burner is brought to test conditions by establishing cooling water and air flow rates, lighting a hydrogen-oxygen fueled ignitor, establishing a pilot level hydrogen flow rate (about 20 percent of the total hydrogen flow required for the test), and establishing the full desired hydrogen and oxygen flows to the heater. Performance plots necessary to determine the relative flow rates of the supply gases for a desired test condition are given in reference 2.

During the typical test time of twelve to fifteen seconds used for the

study reported herein, the rake is injected into the test stream and either gas samples or pitot pressure measurements are made. (Refer to the section on Apparatus and Procedure for details of the gas sample collection and pitot pressure measurement capabilities.) Simultaneous with the rake measurements a computer controlled data scan is performed to define the attained burner test conditions.

For the bulk of the test data acquired to evaluate the different injector configurations the nozzle operated slightly overexpanded. This was purposely done to conserve air and propellants once no apparent effect of burner stagnation pressure was detected on various sets of data. Burner total temperature varied from 2020 K to 2330 K from configuration to configuration, that is, no single value of burner test conditions was employed to study all injectors; however, the variation is not considered broad enough to prevent comparison of the effects of one injector design with another.

## DATA ANALYSIS PROCEDURE

In order to evaluate the gas composition measurements taken from the burner-nozzle exit flow, and thereby determine the adequacy of the burner injectors, it is necessary to account for not only the amount of each gas constituent present, but also its source. (A complete outline of the gas sample data reduction procedure is in Appendix A.) For example, the oxygen measured locally could come from the air supplied or the oxygen supplied to the heater. Therefore, 1 to 2 percent of helium by volume was introduced into the stored oxygen supply. The exact percent of helium was determined from a gas chromatograph analysis of the oxygen. It was then possible to trace the air through the burner by the use of the nitrogen in air, and to trace the oxygen through the burner by the use of the helium. The total oxygen which should be at a local point in the flow, can thus be calculated from the nitrogen and helium measured at a local point. The difference between the calculated and measured oxygen is proportional to the amount of water formed. From the water computed, and the free hydrogen measured the local hydrogen distribution may then be caluclated. It is noted that free hydrogen was not detected for any of the injector configurations, which indicates within measurement accuracy, that complete combustion was obtained.

## RESULTS AND DISCUSSION

### Original Injectors

The original burner injector configuration is shown in figure 3(a). It is seen that the original oxygen injectors consisted of twelve equally spaced injectors on a circle of 6.67 cm radius, all supplied from a common toridal manifold. The twelve hydrogen injectors were equally spaced between the oxygen injectors, but on a circle of 4.6 cm radius. Both injectors consisted of 1.59 cm hex-shaped, flat-faced bodies which exhausted the hydrogen and oxygen parallel to, and in the direction of the air flow. The exit plane of both injectors lay in approximately the same plane. None of the supply gas streams, air, hydrogen,

or oxygen were choked; however, no pressure oscillations were noted for this or any other injector configuration reported herein.

Data from the burner-nozzle exit are presented in figures 3(b), (c), (d) and (e). Figure 3(b) presents the ratio of pitot pressure to burner stagnation pressure laterally across the burner-nozzle exit and at eight vertical locations z/h from 0.2 to 0.87. For this particular data the nozzle is essentially fully expanded, and the measured $P_{t,2}/P_{t,b}$ compares well with a theoretical value of 0.35 which was computed from isentropic flow relations with a representative value of the ratio of specific heats of 1.25. Values of the ratio of measured to theoretical burner stagnation pressure for full nozzle expansion, $\overline{P}_{t,b}$ and theoretical burner total temperature $T_{t,b}$ are given on all data figures. The value of the theoretical burner stagnation pressure used was 2.76 $MN/m^2$ as reported in reference 6 for similar test conditions. The theoretical burner total temperature was computed by the method discussed in Appendix B of reference 2 assuming complete combustion and using an applicable heat loss of 13 to 15 percent of the heat added by combustion. The data band in figure 3(b) shows slightly larger scatter for $y/w > 0$. Evident in these data and essentially all subsequent data, is a higher than average pitot pressure at the left of the figure and a lower than average pitot pressure to the right of the figure. Whether this trend is indicative of asymmetry of the nozzle flow or inaccuracies in pressure measurement is unknown. Considering the wide band of values of z/h represented in the data of figure 3(b) the distribution is quite acceptable.

Figure 3(c) presents the local mass fraction of air divided by the bulk (or average) mass fraction. The data are presented in the unreacted state as computed by the method outlined in Appendix A. Presentation of the data in the unreacted state allows distributions of air, oxygen, and hydrogen to be examined individually to infer how well each injector configuration performs. Values of the ratio of local to bulk mass fractions of unity for air, oxygen, and hydrogen throughout the nozzle exit region corresponds to perfect mixing. Random deviations from unity of a few percent can be expected because of errors in sample collection and sample analysis. Besides the random error, an uncertainty will be associated with measuring the air, hydrogen, and oxygen flow rates, thus effecting the computed bulk mass fraction. Errors in the bulk mass fraction could be expected to shift the local to bulk values up to several percent either side of unity, but uniformly for a given set of test data. Skewed profiles having definitive distributions are not likely to result from either of the above sources of error. No significant nonuniformity in air distribution is apparent in the data of figure 3(c). However; some random scatter and evidence of relatively lower air concentration at z/h of 0.3 and higher air concentration at z/h of 0.9 is noted.

Figure 3(d) presents the local mass fraction of oxygen (from the stored oxygen supply, which excludes the oxygen in the air supply) divided by the bulk oxygen mass fraction. For values of z/h where the air concentration in figure 3(c) is low the oxygen distribution in figure 3(d) appears high relative to unity, and vice versa. This trend is expected as the air and oxygen make up the bulk of the mass of the flow; therefore, a significant local excess of oxygen would be accompanied by a local shortage of air. With the exception of data for

z/h = 3.0, the data indicate slightly lower oxygen concentration in the middle of the flow, y/w near 0.0, with the profile slightly skewed to the left. The low oxygen data point which appears inconsistent (y/w = -0.336, z/h = 0.63) is related to a lower than typical measured helium concentration, and is probably in error.

Figure 3(e) presents the local hydrogen to bulk hydrogen mass fraction ratio. Since no free hydrogen was detected in the gas samples, high hydrogen concentration is indicative of high temperature. The effect of the probe on temperature estimates has been discussed in the section entitled "Gas Sample Collection System." The data suggest a trend of decreasing temperature with increasing z/h. They also show large gradients in temperature, most prominent in the vertical (z direction) short dimension and indicate some large profiling in the lateral (y direction) at z/h of 0.30 and 0.63. Estimates of the temperature range corresponding to the data range from 2090 K for z/h of 0.9 to 2580 K at z/h of 0.3; values are shown on the figure. These temperatures were estimated as discussed in the section entitled "Gas Sample Analysis."

It is noted that the mean of the hydrogen data of figure 3(e) taken over the burner-nozzle exit region is somewhat greater than unity. This effect has been observed for other hydrogen data, as in the final injector configuration discussed later in this report. This indicates experimental error as discussed previously in this section. However, lateral profiling as in the data at z/h of 0.30 and 0.63 is sufficient to demonstrate the unsatisfactory performance of the original injector configuration.

It was concluded a significant temperature profile existed in the two-dimensional burner-nozzle exit flow similar to the profile found in the study of reference 2. Direct comparisons between profiling effects were not attempted because of the different geometries involved. It was noted in reference 2 that only 1/4 of the air flow area was inside the hydrogen injector ring. It was therefore suggested in reference 2 that the temperature profile could be smoothed by relocating the hydrogen injectors. As a result of this suggestion, the number and location of the hydrogen injectors was modified to attempt a more equitable distribution of the hydrogen with respect to the air.

## Thirty-six Tube Hydrogen Injectors

The first modification to the injector system was a thirty-six tube hydrogen injector array as shown in figure 4(a). The geometric arrangement consists of six injectors on a circle of 2.62 cm radius, twelve injectors on a circle of 5.36 cm radius, and eighteen injectors on a circle of 7.82 cm radius. These injectors were spaced such that each injector fueled approximately equal area segments of the burner cross section at the injector location. The injectors were fabricated by brazing 0.138 cm O.D. stainless steel tubing into a pipe nipple which screwed into the original injector fitting. The injector tip shape for this injector modification is shown on figure 4(a). The adapters which converted the original twelve injectors to the thirty-six tube array were sized such that the tips of the hydrogen injectors were approximately 22.8 cm downstream of the oxygen injector exit plane. The exit flow area of the thirty-six

tubes were approximately the same as the original injectors. The oxygen injectors were the same as the original.

Figure 4(b) presents nondimensional pitot pressure distributions at three vertical heights in the nozzle exit. The distributions at the three heights agree well in trend. However, the pitot pressure distribution for $z/h$ of 0.21 is higher than the other data because of operation at a lower burner total pressure. No lateral gradients of consequence are evident in the data.

Figure 4(c) presents nondimensional local to bulk air distributions deduced from the data. Low values are noted on the left side ($y/w < 0$) of the nozzle for $z/h$ of 0.21. The converse is true for the local to bulk oxygen distributions of figure 4(d).

Figure 4(e) presents the deduced local to bulk hydrogen distributions. Surprisingly, the thirty-six tube injectors produced a severe lateral hydrogen gradient at all three vertical locations. Temperature estimates shown on figure 4(e) for the extremes show a temperature gradient of 700 K. Qualitative substantiation for a high temperature at the left of the burner exit, as shown, was evident from visual observation of the heating seen on the pitot-gas sampling rake and other experimental hardware. The reason for the unsatisfactory behavior of the thirty-six tube injector configuration is not fully understood; however, it is observed the thirty-six tube injectors were thin bodies relative to the original blunt-body flat-faced injectors. The thin-body injectors (thirty-six tube configuration) would not have the flame attachment or stabilization characteristics as would the flat-faced injectors. It is suggested that the entire flow pattern within the burner may have been altered depending upon where the flame stabilized within the burner, which depended upon the type of injector used. It is noted that due to the low air velocities in the burner (on the order of 3 to 10 m/sec), the flow would be sensitive to small disturbances. Such disturbances could be associated with the location of the flame within the burner. Conjecture about the difference between the thin- and blunt-body type injectors led to a return to a blunt-faced injector configuration.

## Lengthened-Offset Hydrogen Injectors

This next injector configuration is shown in figure 5(a). It incorporated the blunt-body injector shape of the original injectors with the suggestion of reference 2 that proper radial location of the fuel injectors could eliminate the large temperature profile observed. Significant maldistribution of oxygen had not been observed from the oxygen injectors used, and approximately 50 percent of the air flow passed on each side of the oxygen injector ring which tended to support the argument for radial relocation of the hydrogen injectors. The hydrogen injectors were therefore located on nearly the same diameter as the oxygen injectors but staggered between them. The tips of the hydrogen injectors were about 20.3 cm downstream of the oxygen injector plane, with the original oxygen injectors being used for this configuration.

Typical pitot pressure, local to bulk air, and local to bulk oxygen distributions are shown in figures 5(b), 5(c), and 5(d) for two values of $z/h$. The

pitot data of figure 5(b) show slightly more scatter than the previous two configurations. (See figures 3(b) and 4(b).) The mean level of pitot pressure of figure 5(b) is also near the value (0.4) of the data of figure 4(b) for z/h of 0.21, as expected because the burner nozzle was over-expanded essentially the same amount for both sets of data.

The local to bulk air distribution data of figure 5(c) show a higher degree of uniformity than either of the earlier configurations. (See figures 3(c) and 4(c).) The local to bulk oxygen distributions of figure 5(d) also show good uniformity for z/h of 0.5, but are somewhat less uniform with a left to right gradient for z/h of 0.2.

The local to bulk hydrogen distributions of figure 5(e) unfortunately indicate a sizeable lateral gradient at both vertical locations indicative of a large temperature gradient. Temperature estimates are shown on the figure. The gradient is not as severe as in the thirty-six tube injector data, but is clearly an unsatisfactory distribution. As no satisfactory hydrogen distributions were obtained at this stage of the study, it appeared a more complex heater-injector configuration was necessary.

## Lengthened-Offset Hydrogen Injectors with Baffle

This configuration was identical to the previous configuration with the exception of a baffle installed in the plane of the hydrogen injectors. The configuration is shown in figure 6(a). The baffle was intended to establish an air pressure drop, thus increasing the air velocity and resulting in the establishment of more uniform flow. As the baffle was downstream of the oxygen injectors, a secondary effect was some premixing of the air and oxygen.

Test data pertaining to this configuration are shown in figures 6(b), 6(c), 6(d), and 6(e). Data are shown for two hydrogen injector locations labeled "initial assembly" and "centered"; these labels refer to the position of the injectors within the holes in the baffle plate. The injector position change was accomplished by moving the burner head flange to which the hydrogen manifold is attached. The set of data labeled "initial assembly" will be discussed first. As was the experience with other configurations, no large significant trends are apparent for the local pitot pressure, local to bulk air, or local to bulk oxygen ratio. However, the local to bulk hydrogen distribution of figure 6(e) shows a large gradient. Temperature extremes are shown on the figure.

It was observed that the hydrogen injectors were not well centered in the holes in the baffle plate. The burner head flange was therefore shifted until the best compromise in visual alignment of the injectors was obtained. Data corresponding to this condition are labeled "centered" in figures 6(b) to 6(e). Pitot pressure in figure 6(b) showed no definitive change, but small changes in air (figure 6(c)) and oxygen (figure 6(d)) lateral distributions are evident. However, a dramatic change in the hydrogen distribution shown in figure 6(e) was noted in that the hydrogen gradient completely reversed trends. It was concluded the burner-nozzle exit hydrogen profile was extremely sensitive to the air flow supply distribution through the baffle plate, and also was possibly sensitive

to the uniformity of the mixing of the hydrogen and air-oxygen at each injector. The logical next step was to install spacers on the hydrogen fuel injectors to center each injector in its hole in the baffle plate and thus improve the uniformity of the air-oxygen flow distribution.

## Self-Centering Hydrogen Injectors

The final modification of the hydrogen injectors was to center each injector in baffle plate holes as shown in figure 7(a). An accompanying effect of the spacers shown in figure 7(a) was a net reduction in flow area of approximately 18 percent, with an associated increase in pressure drop across the baffle plate. Pitot pressure distributions are given in figure 7(b) for four vertical locations in the nozzle exit, but no major effect other than over expansion of the nozzle flow and somewhat greater than typical data scatter is evident. It is observed that for all the injector configurations tested, even when severe temperature gradients existed, no significant effect on the pitot pressure distributions was detected.

The local to bulk air distribution is given in figure 7(c) and shows some effect of decreasing air with increasing z/h. Variation between extremes is on the order of ± 3 percent. Compared to the original injectors local to air distribution (see figure 3(c)) the variation has been reduced on the order of 50 percent.

In contrast to the air distribution, the local to bulk oxygen distribution of figure 7(d) shows a trend of increasing oxygen with increasing z/h. The oxygen distribution is also skewed to the right side of the nozzle exit ($y/w > 0$). Variation between extremes is on the order of ± 7 percent. Compared to the original injector local to bulk oxygen distribution (see figure 3(d)), little improvement is noted.

The hydrogen distribution for the self-centering injector configuration is shown in figure 7(e) and varies approximately ± 6 percent between extremes for the entire data range of z/h from 0.2 to 0.8. Comparison to figure 3(e) for the original injector configuration shows the significant improvement in hydrogen distribution; note the variation is around ± 20 percent for the data of figure 3(e) for the original injectors. The hydrogen variation has therefore been improved by a factor of approximately three.

Temperature estimates shown on figure 7(e) for the self-centering injector configuration show differences between the extremes of 150 K as compared to 490 K for the original injector data of figure 3(e). Therefore, the estimated temperature variation has been reduced by a factor slightly greater than three.

Based upon the significant improvement in the air, hydrogen, and deduced temperature distributions relative to the original injectors, and the uncertainties in flow rate and gas sampling measurements, the self-centering injector configuration was considered to produce acceptable burner-nozzle exit profiles.

As the composition profiles and thus deduced temperature distribution are acceptable for the self-centering injector, it is of interest to deduce the Mach number variation from the data of figure 7(b). Using isentropic flow relations

the Mach number variation between extremes is estimated at ±3.2 percent. It is noted the nozzle is over expanded for this data, which may have some effect on the Mach number variation, and clearly has some effect on the Mach number level of the data, as may be seen by comparing the pressure level of figure 7(b) to figure 3(b).

It is observed that the installation of the baffle plate alone, which tended to increase the air velocity and promote premixing of the oxygen and air, was not sufficient to give satisfactory exit profiles. Only by assuring injector alignment with the self-centering injectors in association with the baffle plate, was acceptable burner-nozzle exit profiles obtained. It is suggested, therefore, that the most sensitive phenomenon which affected the profiles was the uniformity of the air distribution supplied to the combustion chamber. Therefore, in the design of combustion burners the designer must recognize the necessity to accept significant air pressure drop to achieve the required uniformity of air distribution.

The final burner injector configuration, relative to the original burner injector configuration, produced significant improvement in uniformity of the air, hydrogen, and deduced temperature distributions in the burner-nozzle exit flow, and insignificant effect upon the oxygen and pitot pressure distribution.

## CONCLUDING REMARKS

As a result of the need for a uniform hot gas test stream for fuel injector development for hydrogen fueled supersonic ramjet combustors, a study of the effect of varying the injector configuration of a hydrogen-fueled, oxygen-replenished combustion burner has been conducted. The purpose of the study was to eliminate an unsatisfactory composition profile, and associated temperature profile observed in the burner-nozzle exit flow. The composition and deduced temperature profiles were reduced to an acceptable level by determining a suitable location for the hydrogen injectors and installing a baffle in the plane of the hydrogen injectors. It was found necessary to redistribute the hydrogen fuel, increase the air pressure drop, promote premixing of the oxygen and air, and establish a uniform flow pattern where the oxygen-air mixture comes into contact with the hydrogen fuel. This was achieved by progressive modification of the burner injector configuration. It is believed the most sensitive phenomenon which affected the composition profiles was the uniformity of the air distribution supplied to the combustion chamber. Therefore, in the design of combustion burners the designer must recognize the necessity to accept significant air pressure drop to achieve the required uniformity of air distribution.

Relative to the original burner injector configuration, the final injector configuration produced significant improvement in uniformity of the air, hydrogen, and deduced temperature distributions in the burner-nozzle exit flow, and insignificant effect upon the oxygen and pitot pressure distributions. In addition, the pitot pressure distribution was found to be insensitive to severe gradients in hydrogen composition and temperature. This fact emphasizes the necessity for local gas composition measurements in order to assess the uniformity and acceptability of combustion burner performance.

APPENDIX A

## Gas Sample Data Reduction Procedure

The purpose of the gas sample measurements was to evaluate how uniformly the various injector configurations distributed the gases at the burner-nozzle exit. As shown in the following simplified burner schematic, gas supplied to the burner comes from three separate sources and consists of air, hydrogen, and oxygen, the latter containing helium tracer.

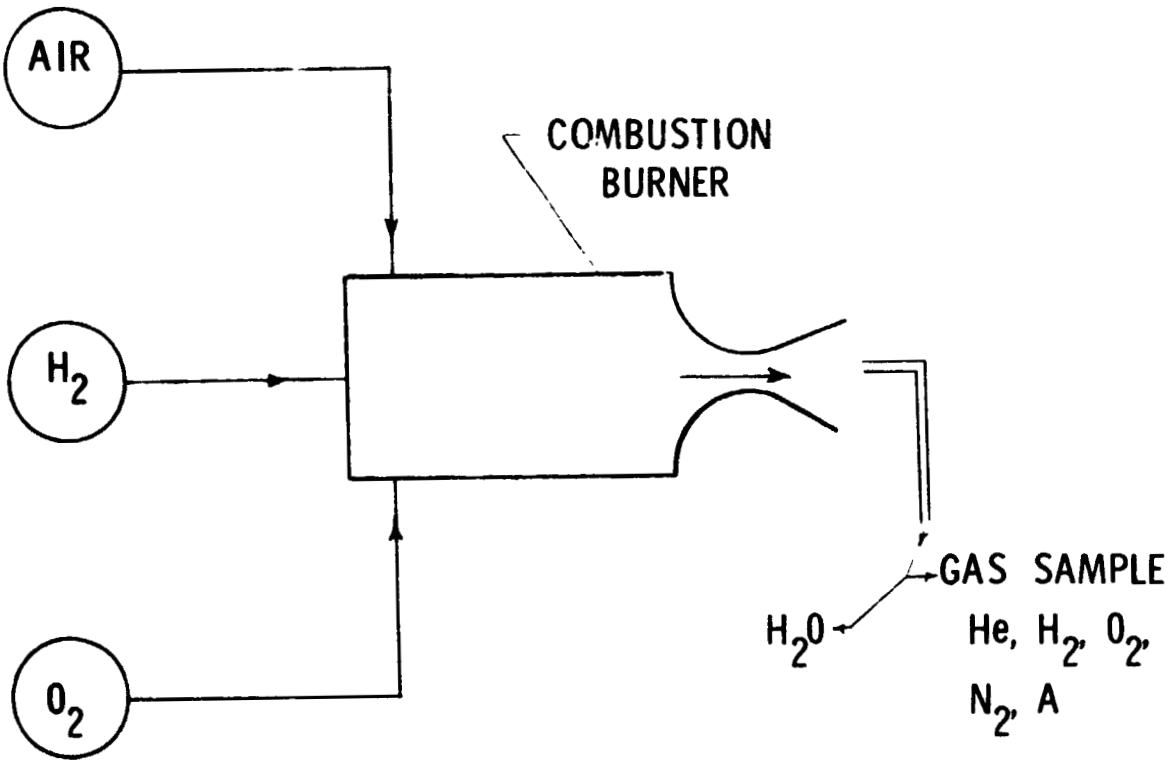


BURNER SCHEMATIC

In order to distinguish between the oxygen from the air and the oxygen supplied from the storage vessel, approximately 1 percent of helium by volume was added to the stored oxygen. In this Appendix, the latter source of oxygen will be referred to an oxidant. The distinction between oxidant and pure oxygen is not made in the main body of this report as the difference in terms of local to bulk mass fraction ratio is insignificant. The oxidant contains oxygen, the added helium, and trace amounts of nitrogen as an impurity. The helium serves to identify the oxidant distribution and the nitrogen in the air serves to identify the air distribution at the burner-nozzle exit through the use of the gas sample measurements.

As noted in the section entitled Apparatus and Procedure and illustrated on the burner schematic, water condensed from the gas samples. Therefore, the gas sample collection and analysis result is mole fractions of helium, hydrogen, oxygen, nitrogen, and argon on a dry basis. That is, the samples did not directly account for the water content of the test gas from the burner. However, the water distribution and therefore the hydrogen distribution at the burner-nozzle exit is computable from other gas sample measurements because of the use of the helium tracer in the oxidant supply. Conversion of the gas sample dry analysis to a wet basis (which includes water) is performed by a computerized data reduction program.

For each gas sample the mole fraction of water is computed by the following procedure: by use of the helium tracer the local amount of oxygen from the oxidant is determined. Similarly, by use of the nitrogen, the oxygen from air which should be at a point is determined. The difference between the computed oxygen from the two sources, and the measured free oxygen has reacted to water. The equations used are as follows, where first the mole fraction of oxidant and air are computed. The local mole fraction of oxidant $\beta_o$ is given by equation 1.

$$\beta_o = \frac{N_{he}}{C_{he}} \qquad \text{(dry basis)} \qquad (1)$$

In equation 1, $N_{he}$ is the mole fraction of helium from the dry gas sample analysis and $C_{he}$ is the mole fraction of helium in the oxidant supply. Similarly, the local mole fraction of air, $\beta_a$ is given by equation 2.

$$\beta_a = \frac{N_n - \beta_o C_n}{A_n} \qquad \text{(dry basis)} \qquad (2)$$

In equation 2, $N_n$ is the mole fraction of nitrogen from the dry gas sample analysis; $\beta_o$ is defined by equation 1; $C_n$ is the mole fraction of nitrogen in the oxidant; and $A_n$ is the mole fraction of nitrogen in air. From the results of equations 1 and 2 the mole fraction of water, $N_w$ (the units of $N_w$ are moles of water per mole of dry gas mixture) is given by equation 3.

$$N_w = (\beta_a A_o + \beta_o C_o - N_o) \qquad \text{(dry basis)} \qquad (3)$$

In equation 3, $\beta_o$ and $\beta_a$ are from equations 1 and 2, respectively; $A_o$ is the mole fraction of oxygen in air; $C_o$ is the mole fraction of oxygen in the oxidant; and $N_o$ is the local oxygen mole fraction from the dry gas analysis. The factor "2" comes from the fact that one mole of oxygen forms two moles of water. To complete conversion of the dry gas sample analysis to a wet basis, the water mole fraction computed in equation 3 is added into the dry gas mixture. The sum of the mole fractions S, is given by equation 4.

$$S = N_w + N_h + N_o + N_n + N_A + N_{he} \qquad (4)$$

In equation 4, $N_w$ is from equation 3, and the remaining terms are mole fractions of hydrogen, oxygen, nitrogen, argon, and helium which are the results of the dry gas sample analysis. The mole fraction of each constituent on a wet basis is therefore the mole fraction of each constituent as given in the individual terms of equation 4, divided by the sum S. For example, the mole fraction of oxygen on a wet basis $N_{o,w}$ is given by equation 5.

$$N_{o,w} = \frac{N_o}{S} \qquad \text{(wet basis)} \qquad (5)$$

Similarly, all other mole fractions on a wet basis may be computed thus determining the gas constituents of interest in the test gas stream.

For purposes of examining the injector performance in the burner, it is desirable to examine the distributions of air, oxidant, and hydrogen in the burner-nozzle exit. Since each of these gases is associated with a particular supply and injector configuration, maldistribution of a particular gas may give a clue as to what injector modification is required. The local oxidant and air mole fraction have already been determined from the gas analysis results as given by equations 1 and 2. It remains to compute the hydrogen concentration from the measured free hydrogen and the hydrogen in the computed water, and form the new mole fractions for the mixture of hydrogen, air, and oxidant.

Recognizing that one mole of hydrogen reacts to form one mole of water, the hydrogen mole fraction $\beta_h$ is given by equation 6.

$$\beta_h = N_h + N_w \qquad \text{(dry basis)} \qquad (6)$$

In equation 6, $N_h$ is the hydrogen mole fraction from the dry gas sample analysis and $N_w$ is given by equation 3. For the unreacted gas mixture at the burner-nozzle exit the local air $\beta_{a,\ell}$, local oxidant $\beta_{o,\ell}$, and local hydrogen $\beta_{h,\ell}$, mole fractions are given by equations 7, 8, and 9, respectively.

$$\beta_{a,\ell} = \frac{\beta_a}{\beta_a + \beta_o + \beta_h} \tag{7}$$

$$\beta_{o,\ell} = \frac{\beta_o}{\beta_a + \beta_o + \beta_h} \tag{8}$$

$$\beta_{h,\ell} = \frac{\beta_h}{\beta_a + \beta_o + \beta_h} \tag{9}$$

In equations 7, 8, and 9, $\beta_a$ is given by equation 2, $\beta_o$ by equation 1, and $\beta_h$ by equation 6. The conversion of the mole fractions, given by equations 7, 8, and 9, to mass fraction requires use of the mixture molecular weight $M_m$ given by equation 10.

$$M_m = M_a\beta_{a,\ell} + M_o\beta_{o,\ell} + M_h\beta_{h,\ell} \tag{10}$$

In equation 10, $M_a$, $M_o$, and $M_h$ are the molecular weights of air, oxidant, and hydrogen, respectively. The local mass fractions of air $\alpha_{a,\ell}$, oxidant $\alpha_{o,\ell}$, and hydrogen $\alpha_{h,\ell}$ are given by equations 11, 12, and 13, respectively.

$$\alpha_{a,\ell} = \frac{M_a}{M_m}\beta_{a,\ell} \tag{11}$$

$$\alpha_{o,\ell} = \frac{M_o}{M_m}\beta_{o,\ell} \tag{12}$$

$$\alpha_{h,\ell} = \frac{M_h}{M_m}\beta_{h,\ell} \tag{13}$$

A measure of how evenly a particular burner injector configuration distributes each gaseous component, is the ratio of the local mass fractions given by equations 11, 12, and 13 to the bulk mass fractions. The bulk mass fractions of air $\alpha_a$, oxidant $\alpha_o$, and hydrogen $\alpha_h$ may be calculated from the metered flow rates to the burner as follows:

$$\alpha_a = \frac{m_a}{m_h + m_o + m_a} \tag{14}$$

$$\alpha_o = \frac{m_o}{m_h + m_o + m_a} \tag{15}$$

$$\alpha_h = \frac{m_h}{m_h + m_o + m_a} \tag{16}$$

In equations 14, 15, and 16, $m_n$, $m_o$, and $m_a$ are the measured mass flow rates of hydrogen, oxidant, and air to the burner, respectively. The local to bulk mass fraction ratios of air $\bar{\alpha}_a$, oxidant $\bar{\alpha}_o$, and hydrogen $\bar{\alpha}_h$ are given by equations 17, 18, and 19, respectively.

$$\bar{\alpha}_a = \frac{\alpha_{a,\ell}}{\alpha_a} \tag{17}$$

$$\bar{\alpha}_o = \frac{\alpha_{a,\ell}}{\alpha_o} \tag{18}$$

$$\bar{\alpha}_h = \frac{\alpha_{h,\ell}}{\alpha_h} \tag{19}$$

Note, the distinction between oxygen and oxidant, the latter of which contains the helium tracer and possible trace amounts of nitrogen, is not made in the main body or figures of this report, as the difference in terms of local to bulk mass fraction ratios is insignificant.

The gas analysis results reported herein are given in the form of the unreacted local to bulk mass fraction ratios, as given by equations 17, 18, and 19. The ideal injector configuration in association with negligible experimental error, would result in values of unity for the local to bulk ratios for all locations in the burner-nozzle exit flow. Discussion of the effects which may cause the local to bulk ratios to deviate from unity, may be found in the section entitled "Results and Discussion".

## APPENDIX B

### Chromatograph Parameters

Separation of the gas samples into components of helium, hydrogen, oxygen, and nitrogen was accomplished by passing the sample through a gas chromotograph setup. Pertinent information on the setup is as follows:

Column - 7.6 m long, 0.23 cm internal diameter

Adsorbent - Molecular sieve type 13X, 30/60 mesh

Carrier Gas - Argon, 38 cc/minute

Detector - Thermistor

Column Temperature - 315 K

Gas Injector Volume - Approximately 2 cc

Analysis Time - 6 minutes

A 0.30 m long, 0.46 cm internal diameter molecular sieve section was installed ahead of the column to absorb any trace of moisture in the gas sample. This section was replaced periodically and served to protect the column, as molecular sieve columns deteriorate rapidly when exposed to moisture. The length of the column was dictated by the requirement to separate helium and hydrogen, which is a relatively difficult separation to attain.

## REFERENCES


1. Anon.: Engineering Analyses and Design Calculation of NASA-Langley Research Center Hydrogen-Air-Vitiated Heater with Oxygen Replenishment. Tech. Memo. No. 173, General Applied Science Labs., Inc., 1974. (Available as NASA CR-132381.)

2. Russin, William Roger: Performance of a Hydrogen Burner to Simulate Air Entering Scramjet Combustors. NASA TN D-7567, 1974.

3. Cohen, Leonard S.; and Guile, Roy N.: Investigation of the Mixing and Combustion of Turbulent, Compressible Free Jets. NASA CR-1437, 1969.

4. Lengelle, G.; and Verdier, C.: Gas Sampling and Analysis in Combustion Phenomena. AGARD-AG-168, pp. 33-54, July 1973.

5. McNair, H. M.; and Boneli, E. J.: Basic Gas Chromatography, Fifth Ed., Consolidated Printers, Copyright 1968.

6. Rogers, R. C.; and Eggers, J. M.: Supersonic Combustion of Hydrogen Injected Perpendicular to a Ducted Vitiated Airstream. AIAA Paper No. 73-1322, Nov. 1973.

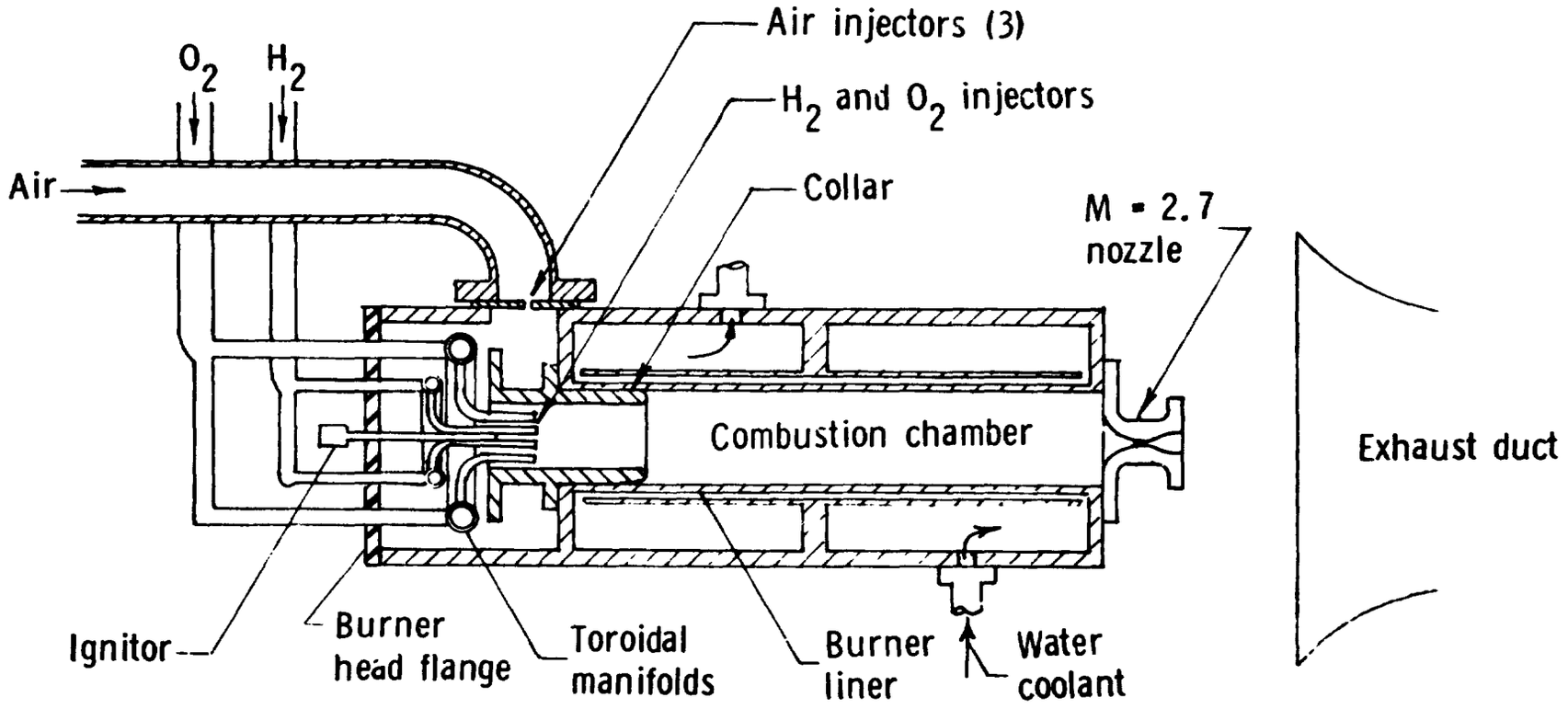


Figure 1.- Combustion burner schematic.

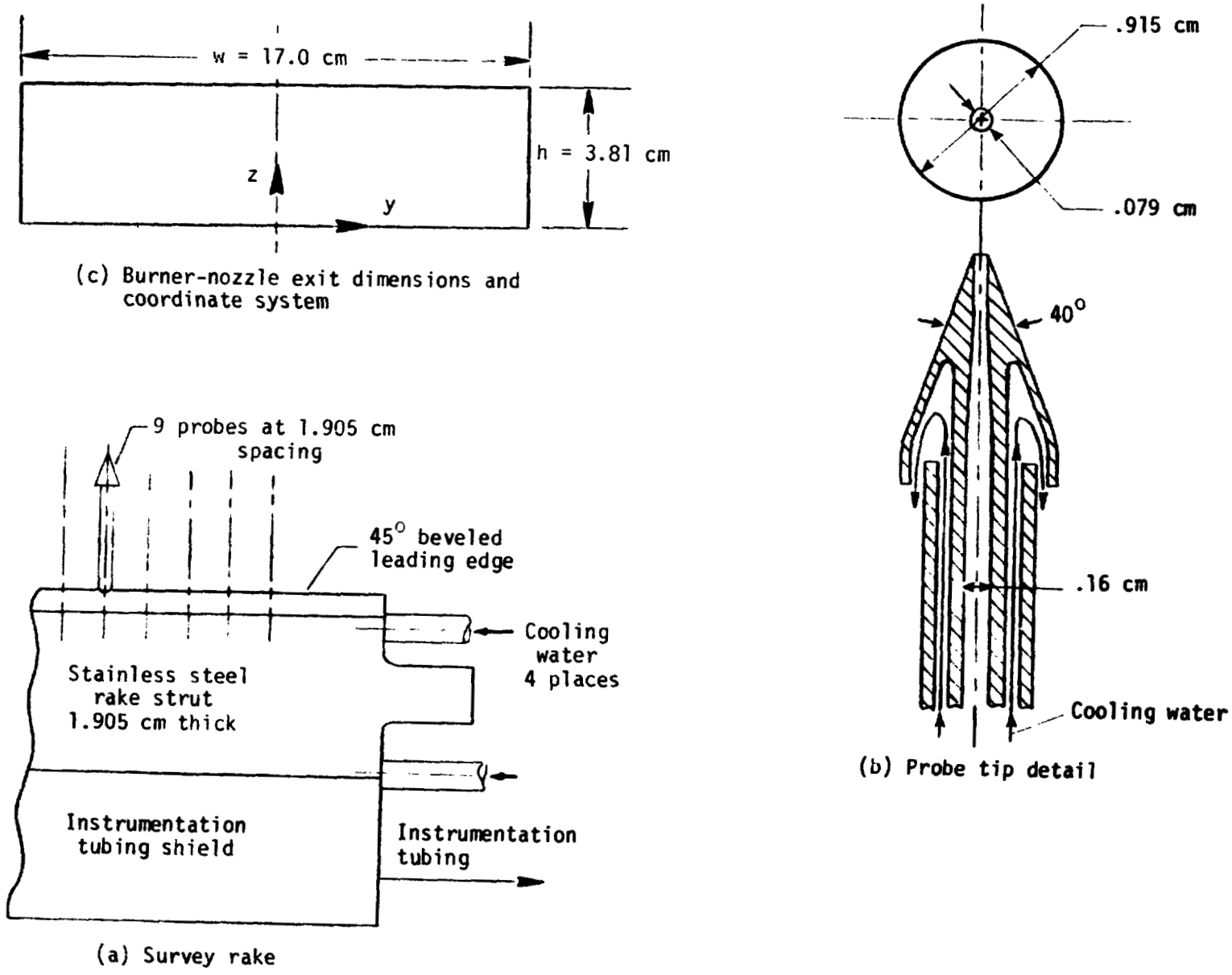


Figure 2.- Survey rake, probe tip detail and combustion-burner-nozzle exit dimensions and coordinate system.

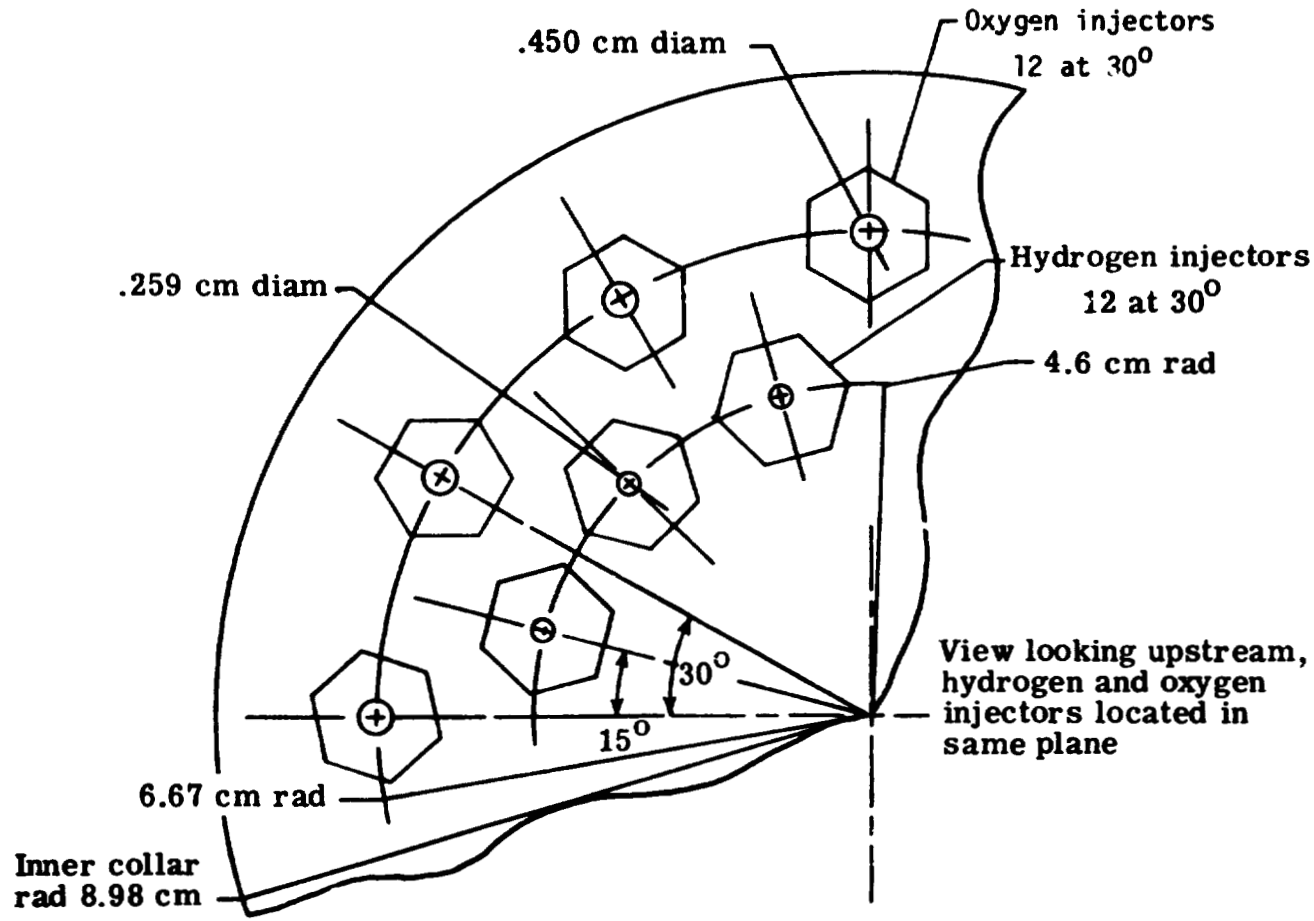


(a) Original injector configuration

Figure 3.- Burner original injector configuration and reduced survey data.

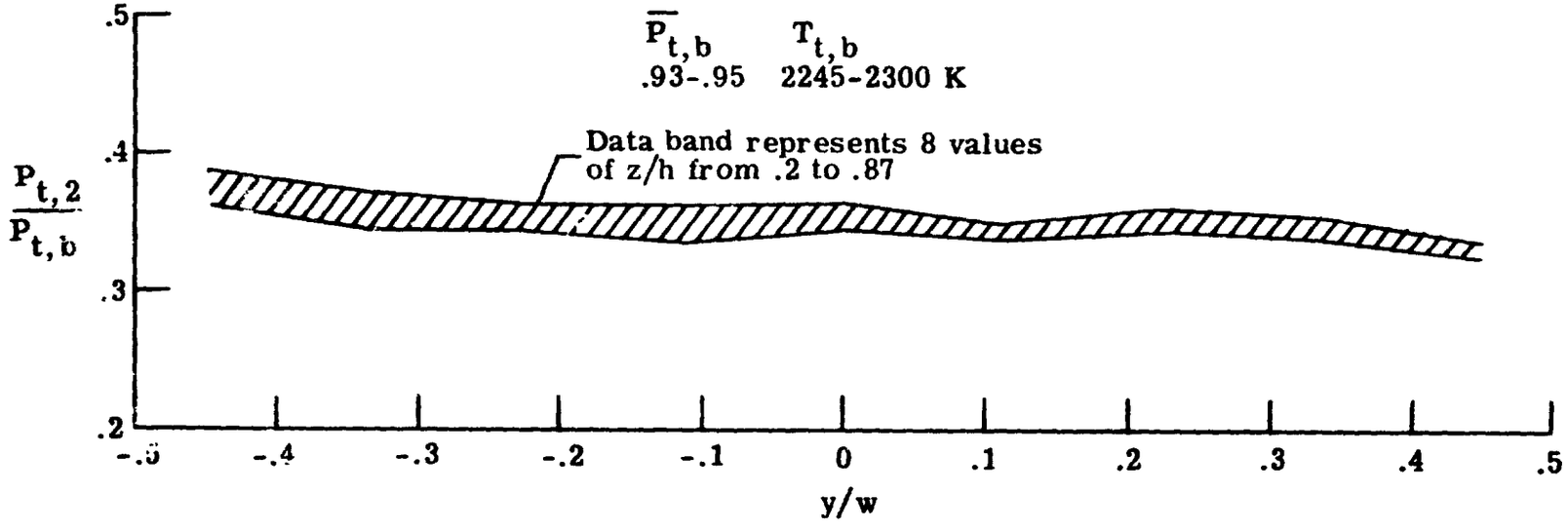


(b) Non-dimensional pitot pressure distribution

Figure 3.- Continued

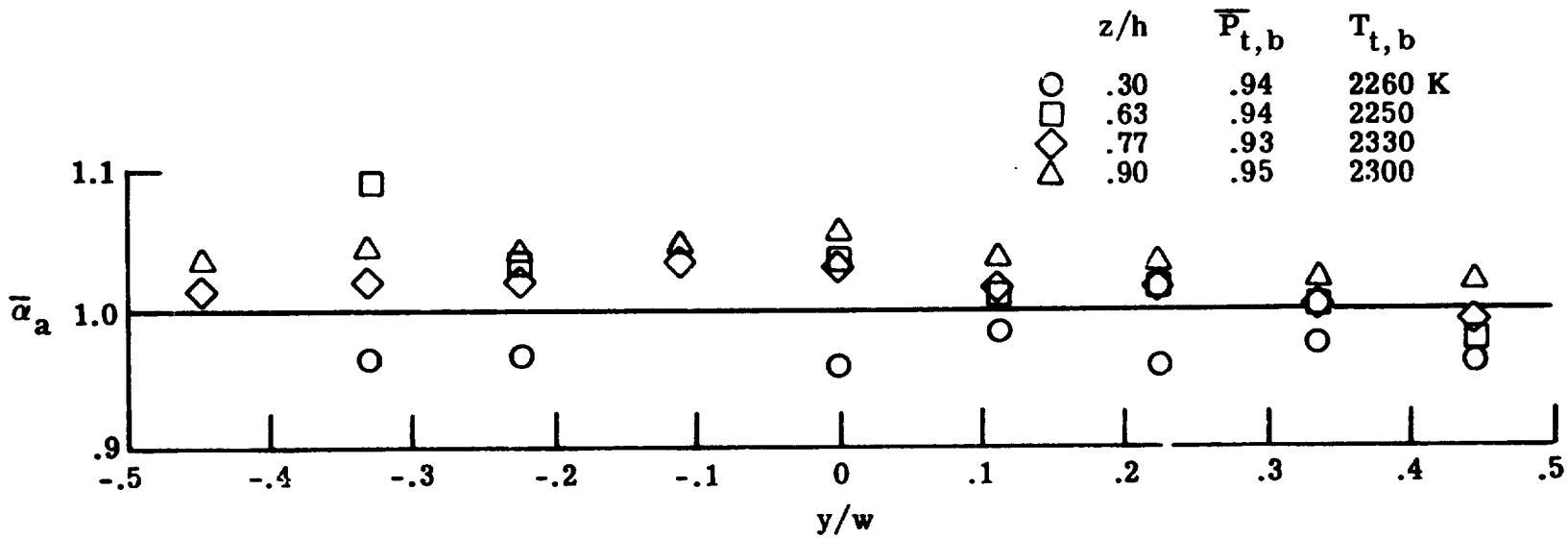


(c) Local to bulk air distribution ratio

**Figure 3.- Continued**

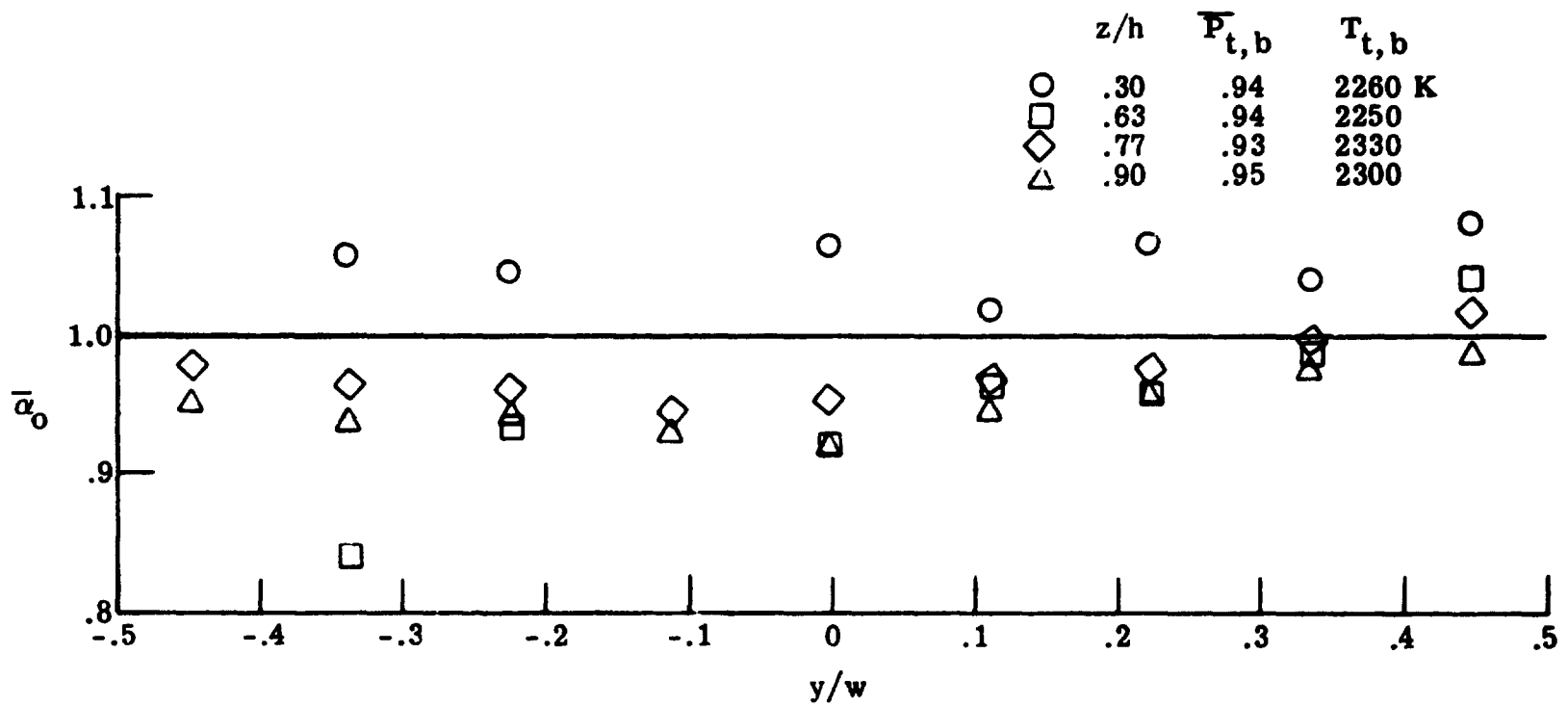


(d) Local to bulk oxygen distribution ratio

Figure 3.- Continued

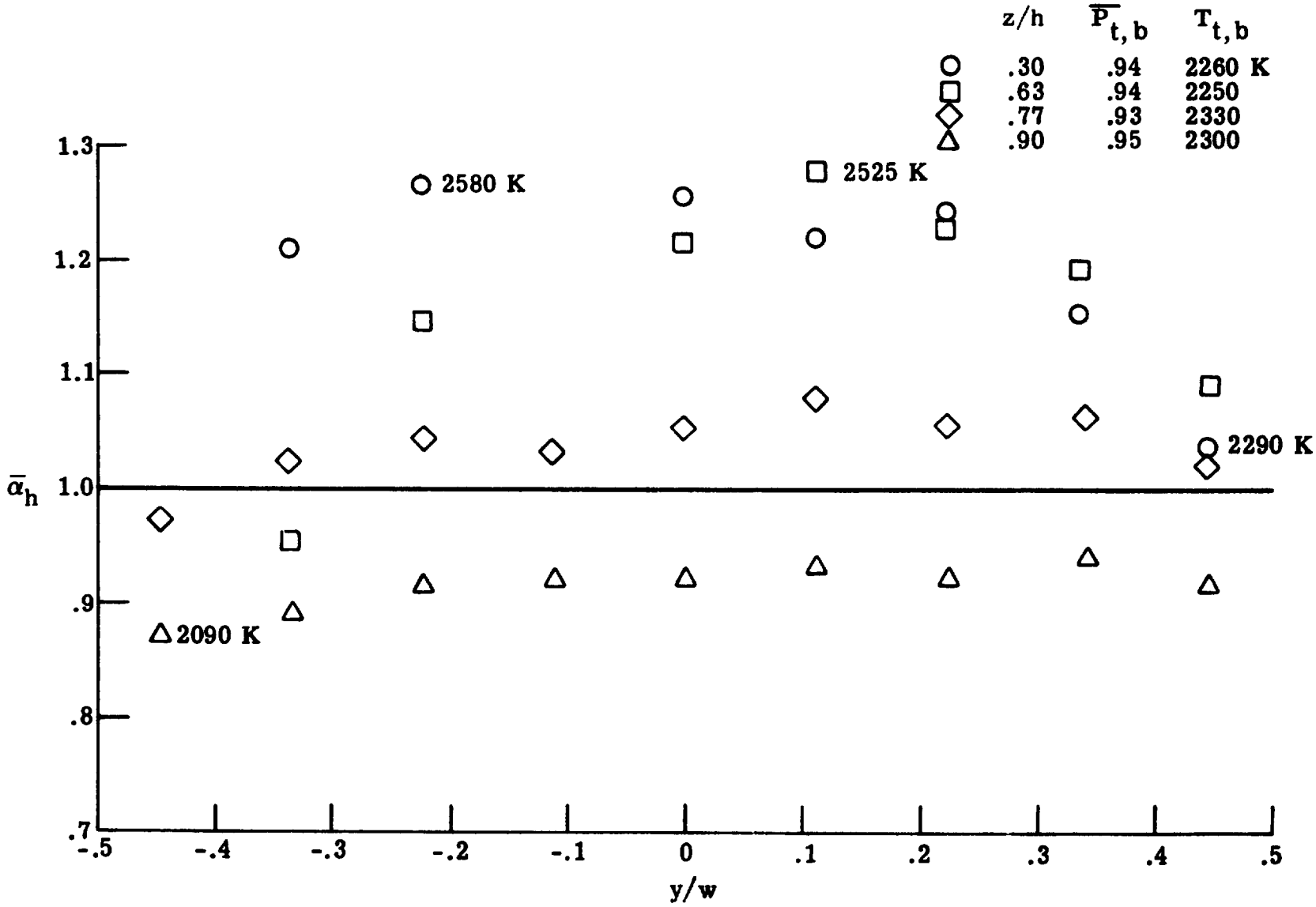


(e) Local to bulk hydrogen distribution ratio

Figure 3.- Concluded

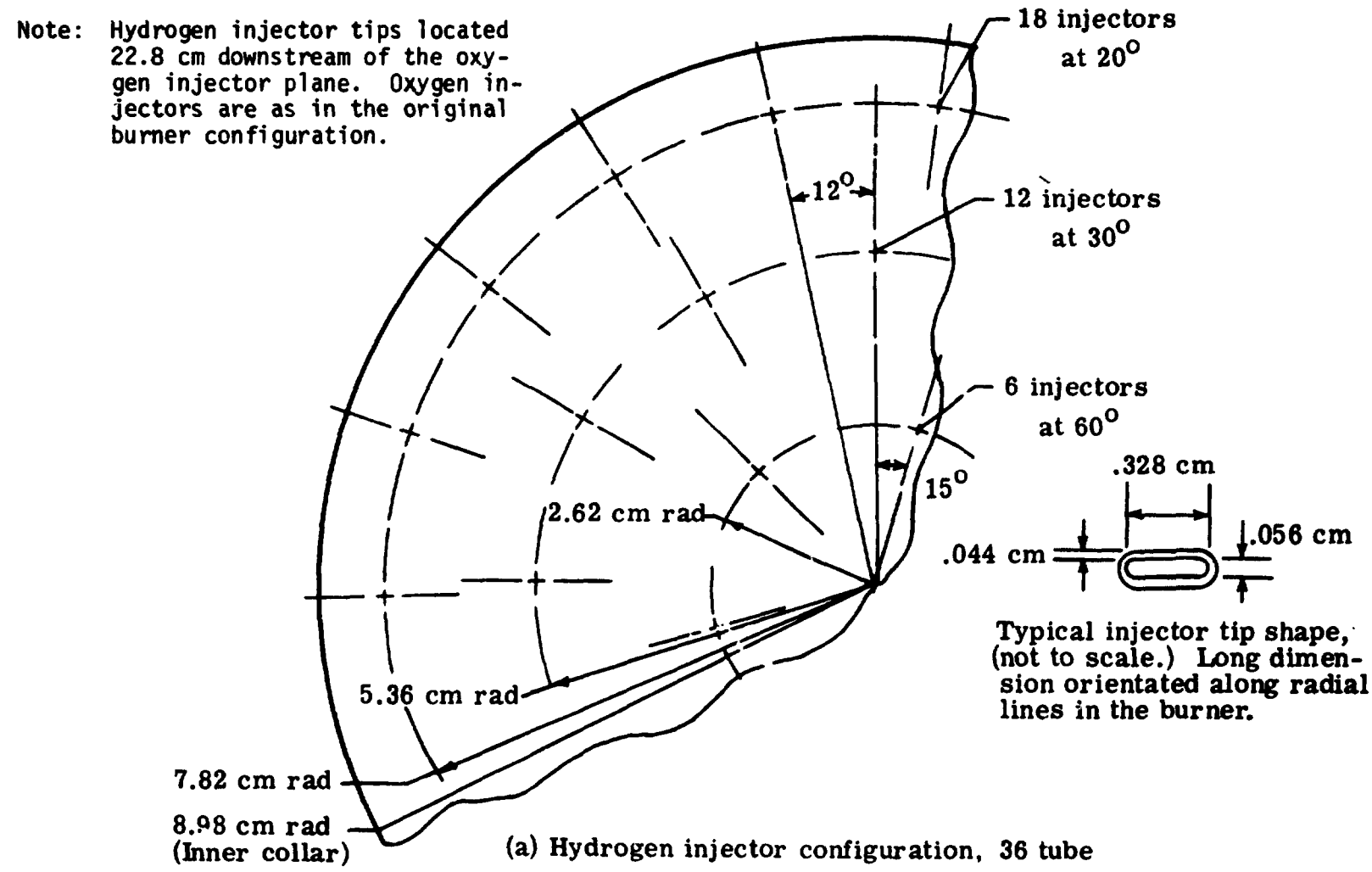


(a) Hydrogen injector configuration, 36 tube

Figure 4.- Burner-hydrogen injector 36 tube configuration and reduced survey data.

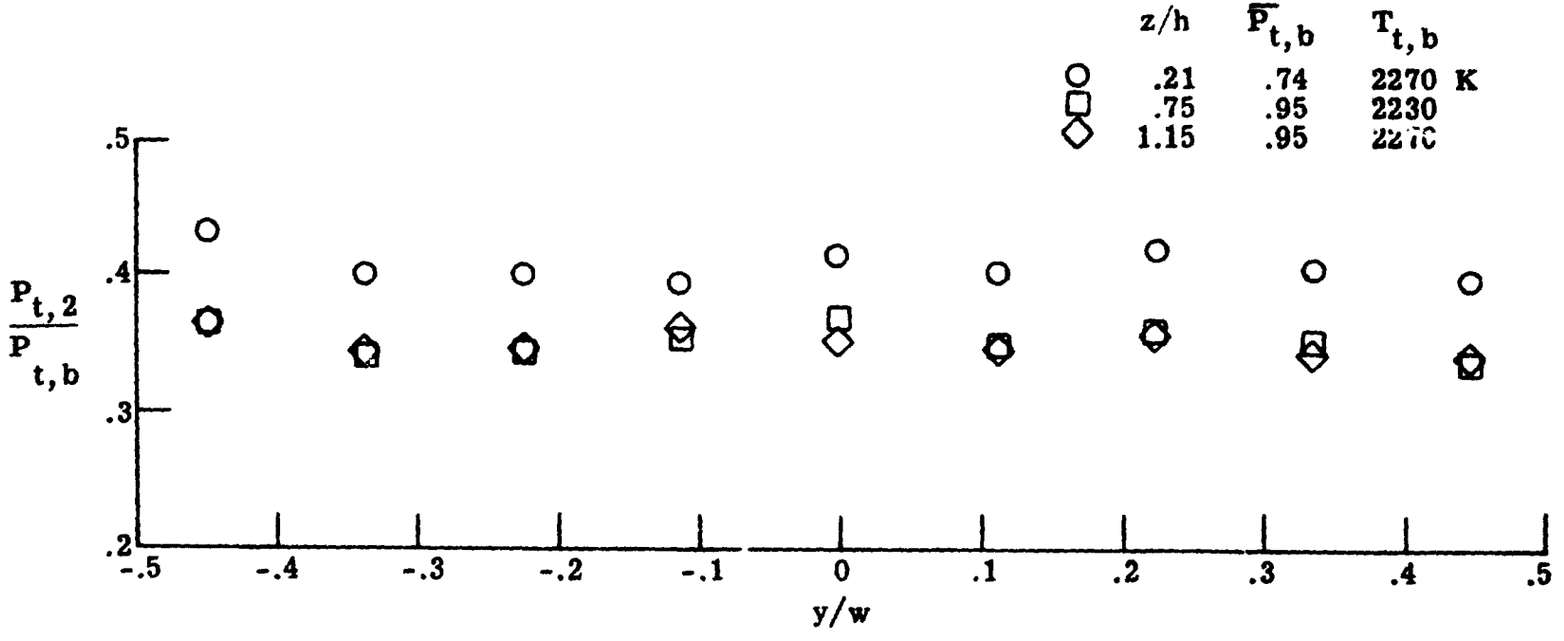


(b) Non-dimensional pitot pressure distribution

Figure 4.- Continued

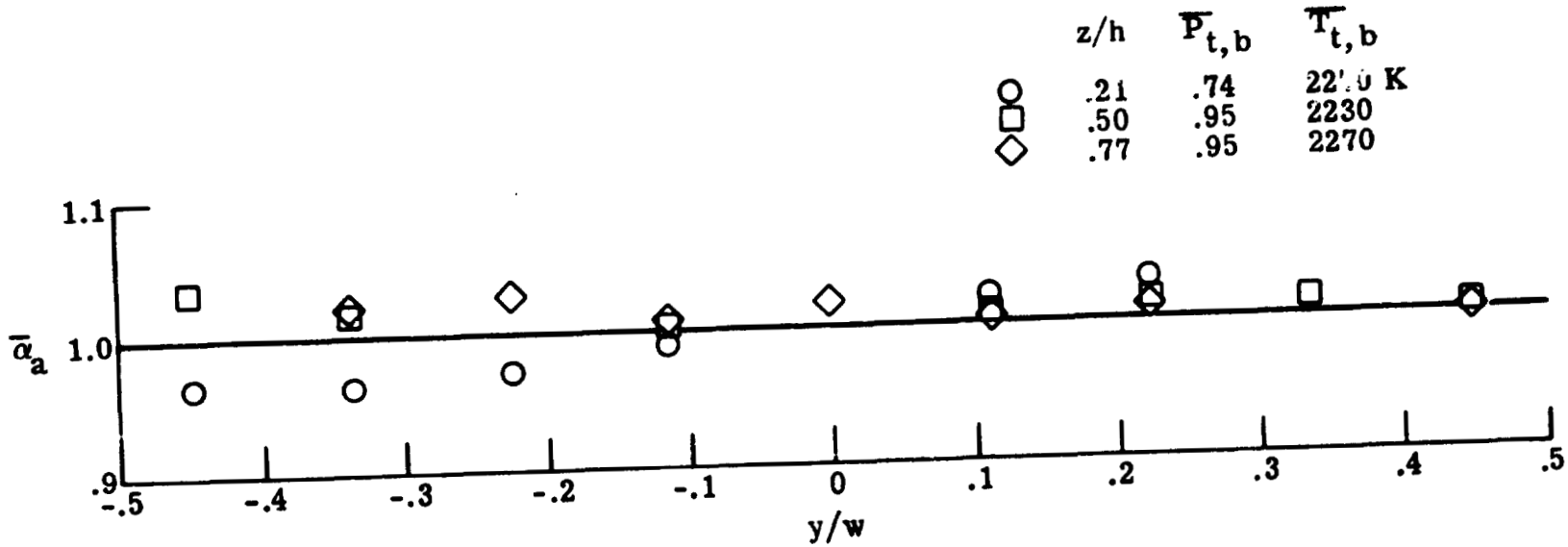


(c) Local to bulk air distribution ratio

Figure 4.- Continued

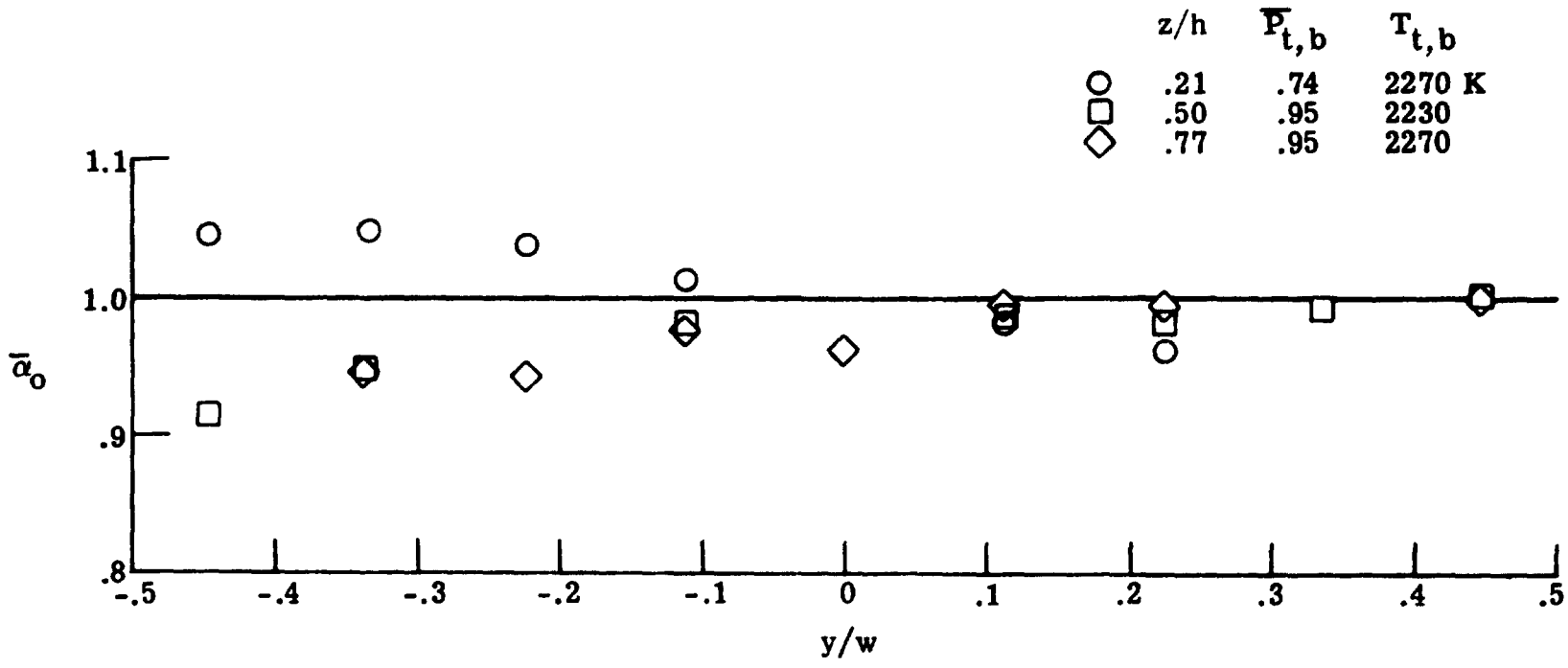


(d) Local to bulk oxygen distribution ratio

Figure 4.- Continued

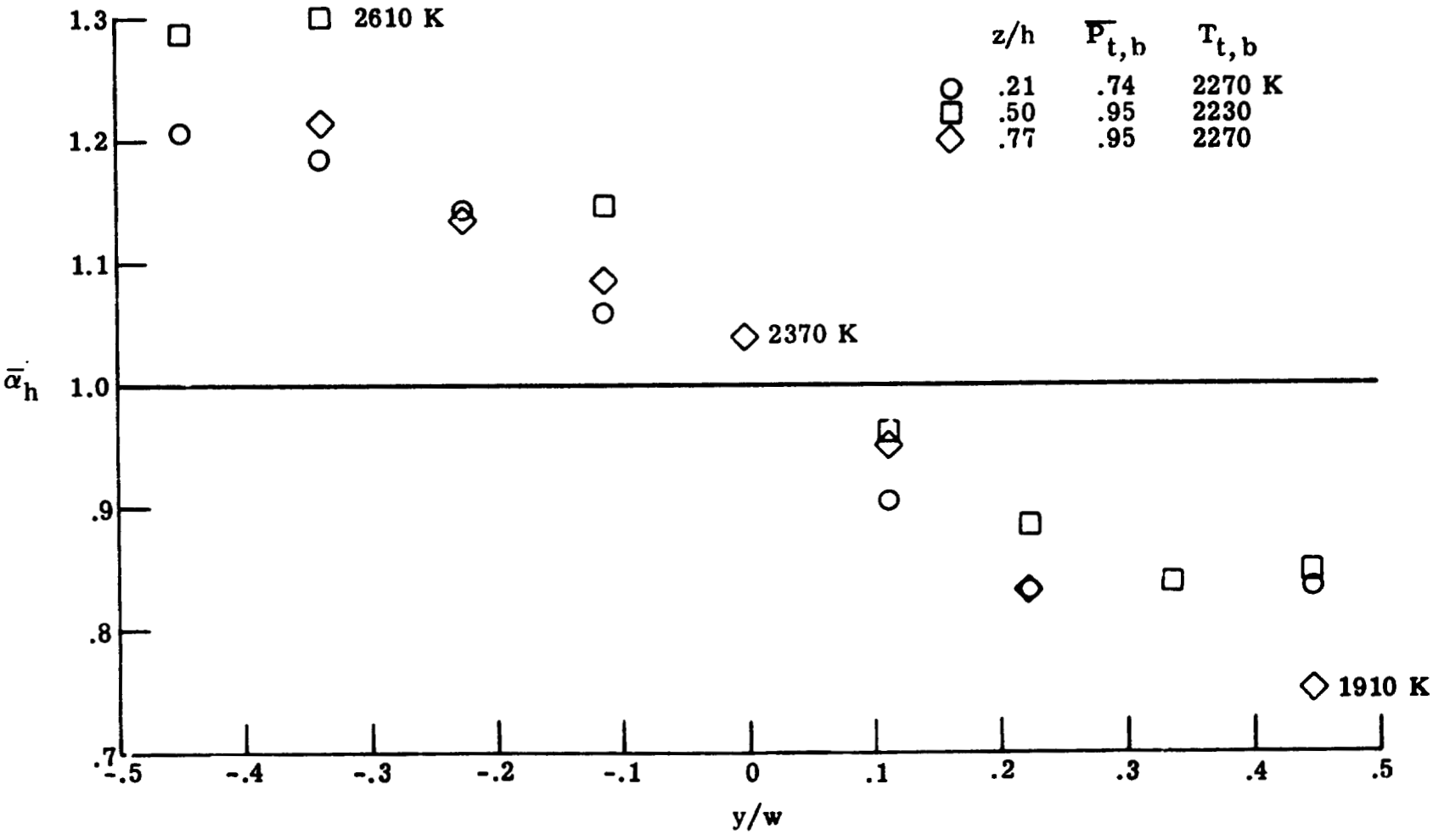


(e) Local to bulk hydrogen distribution ratio

Figure 4.- Concluded

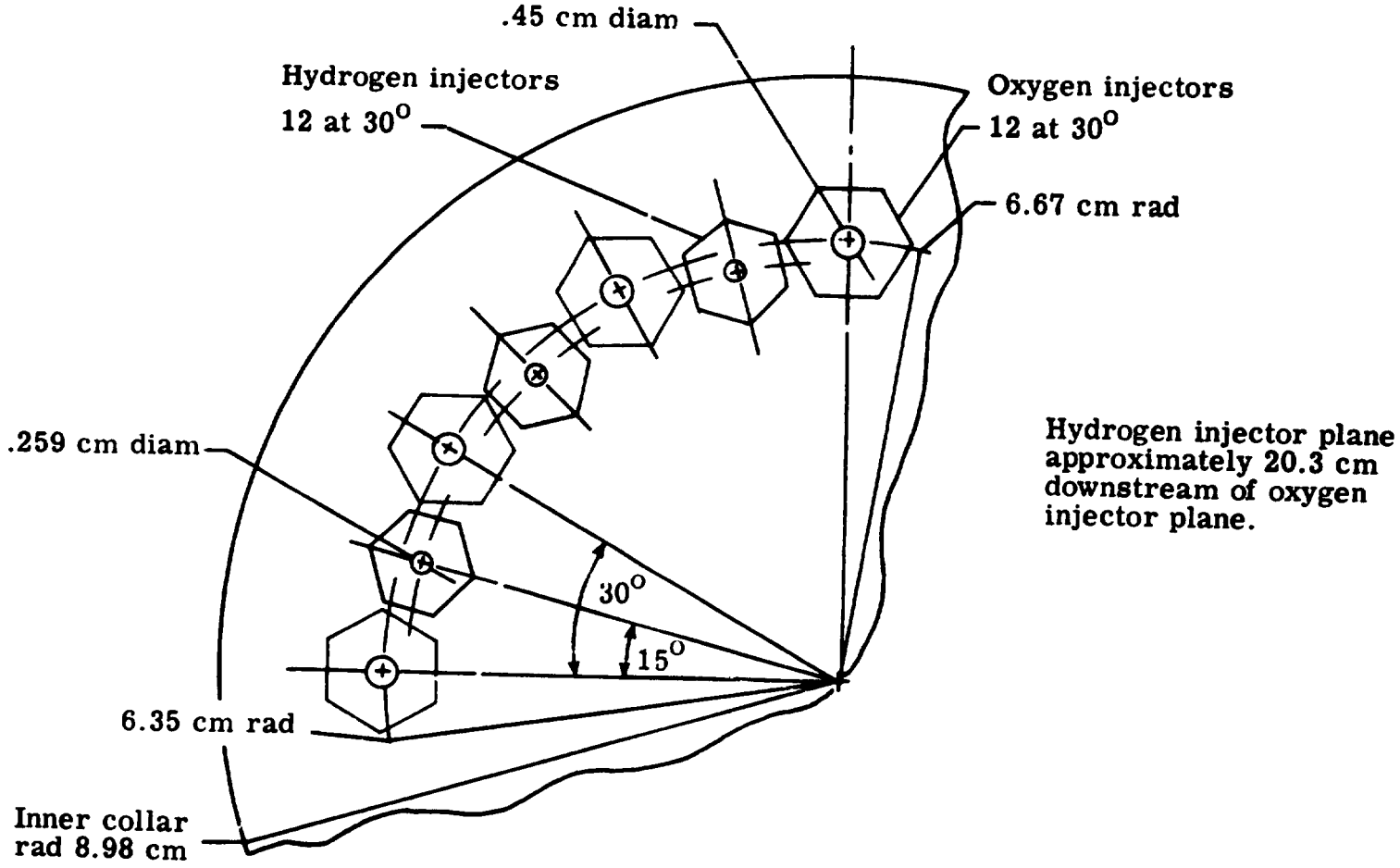


(a) Injector configuration

Figure 5.- Burner injector configuration with hydrogen injectors off-set and extended and reduced survey data.

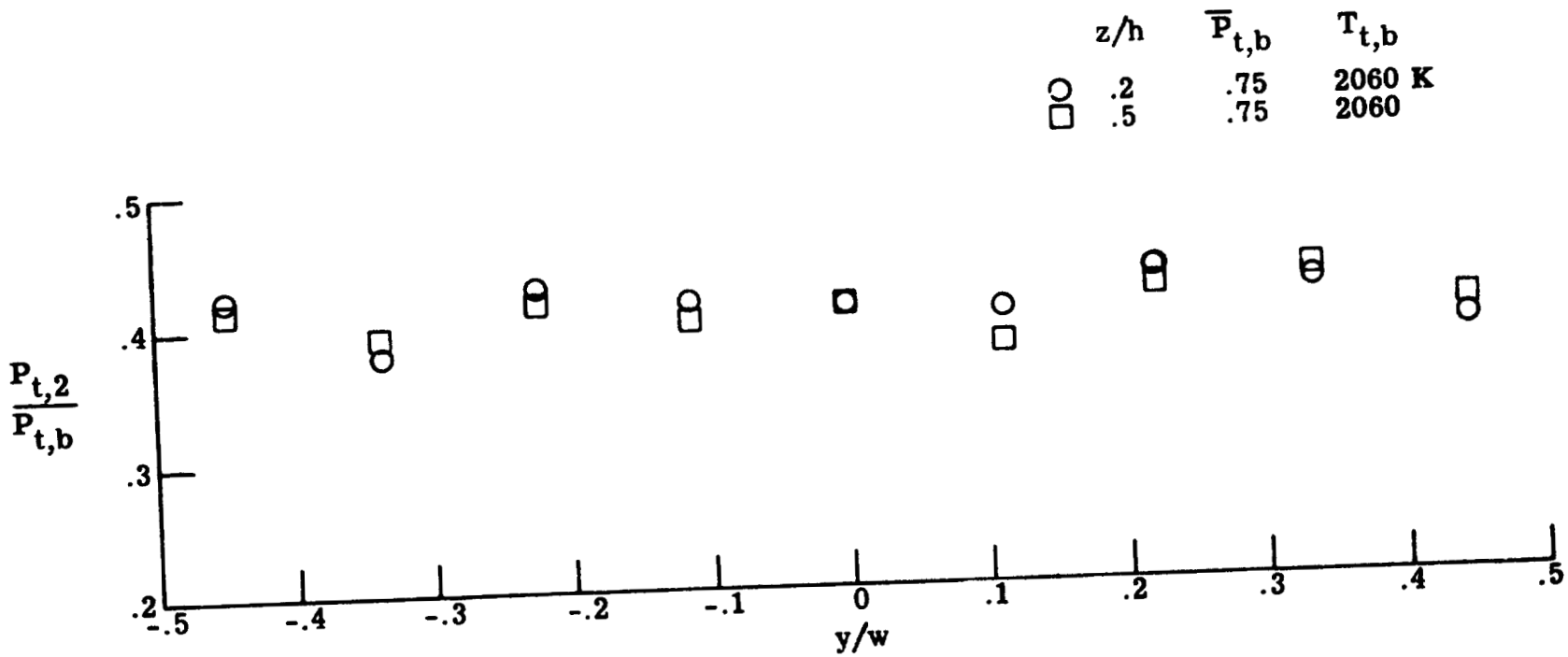


(b) Non-dimensional pitot pressure distribution

Figure 5.- Continued

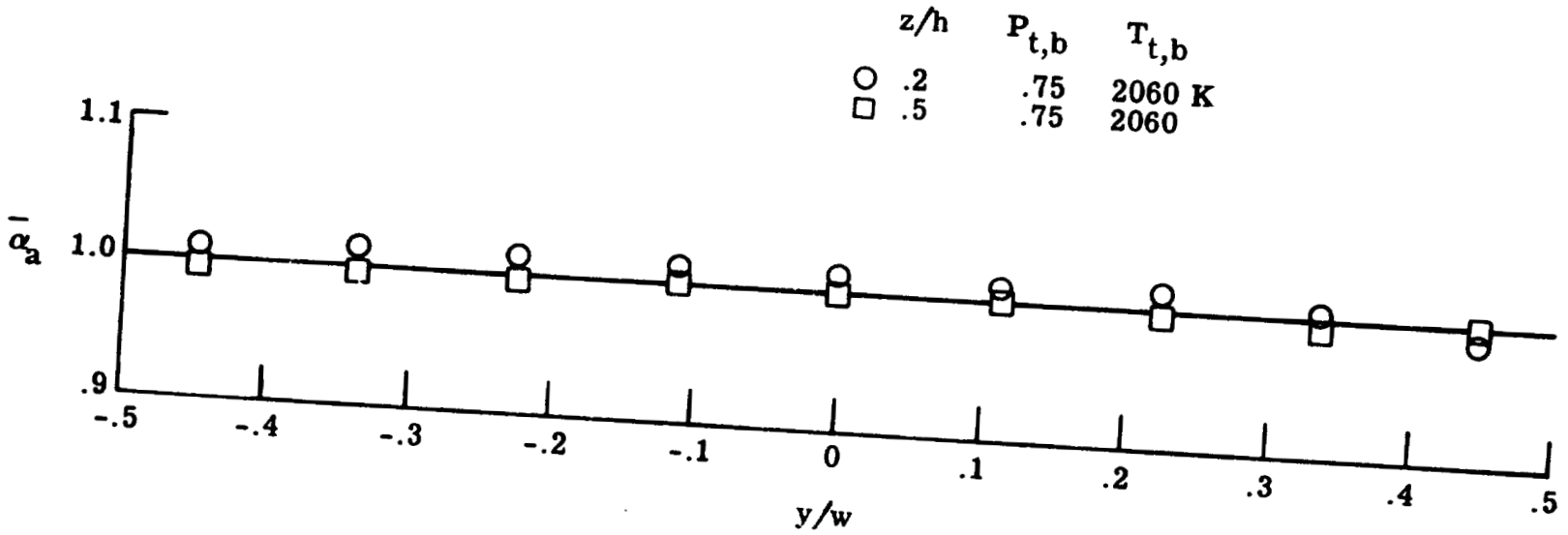


(c) Local to bulk air distribution ratio

Figure 5.- Continued

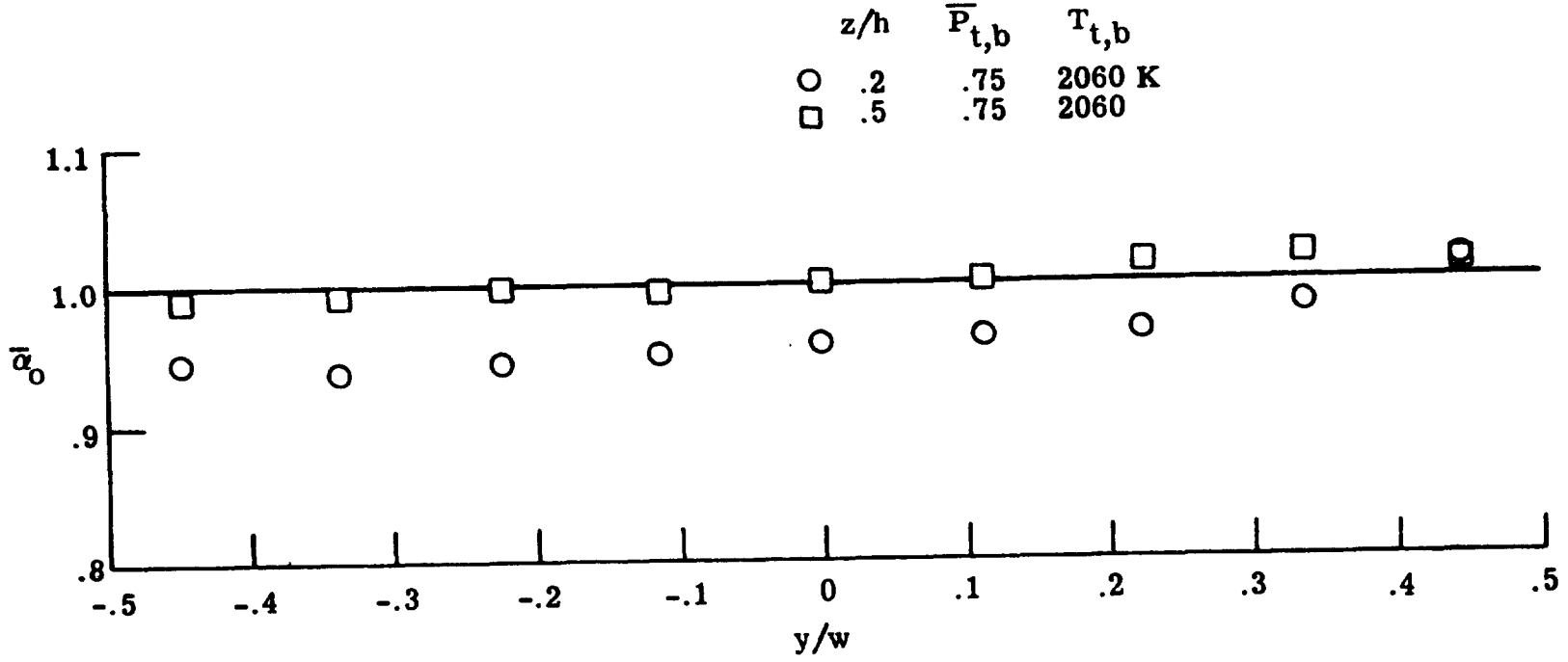


(d) Local to bulk oxygen distribution ratio

Figure 5.- Continued

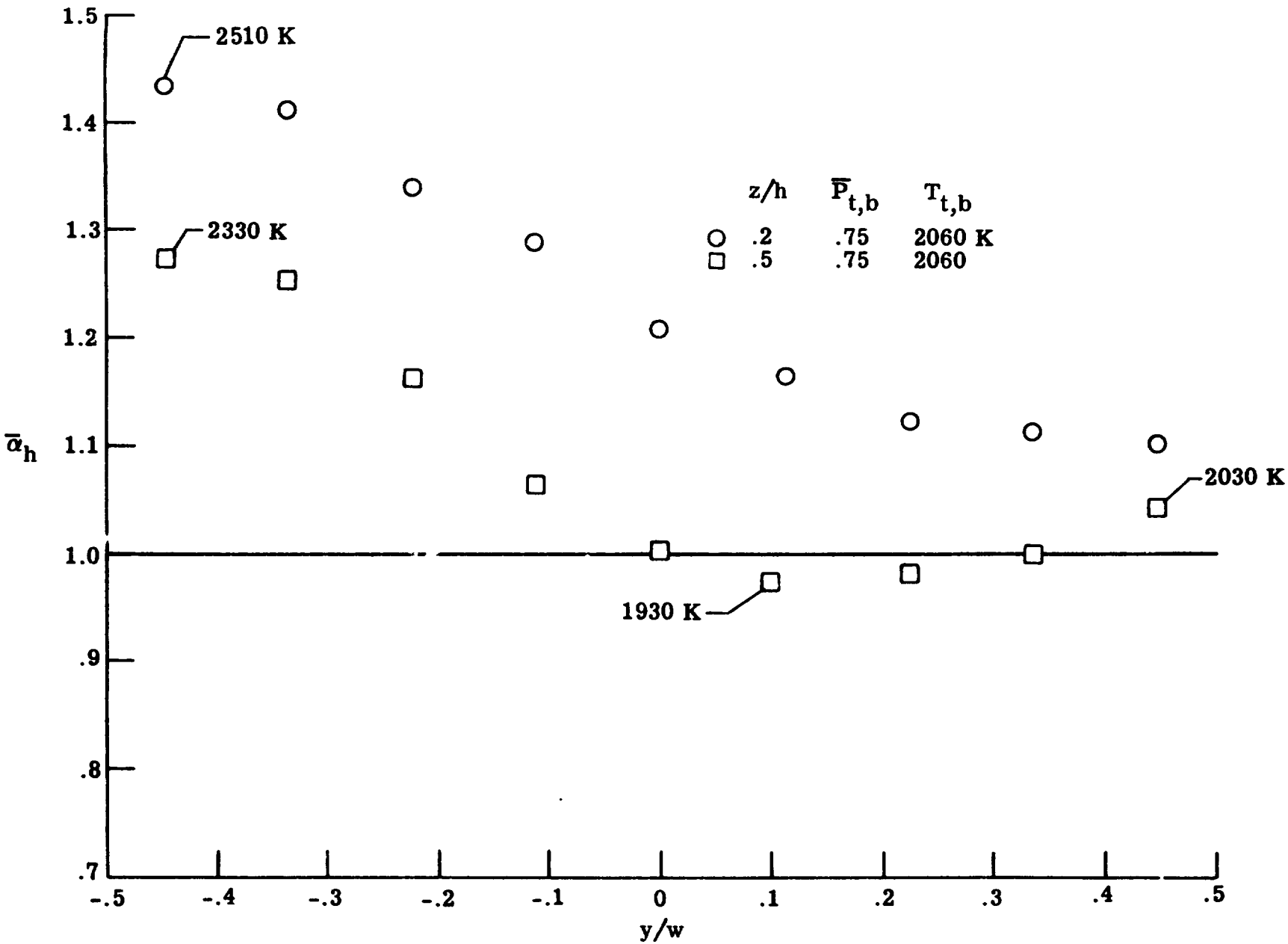


(e) Local to bulk hydrogen distribution ratio

Figure 5.- Concluded

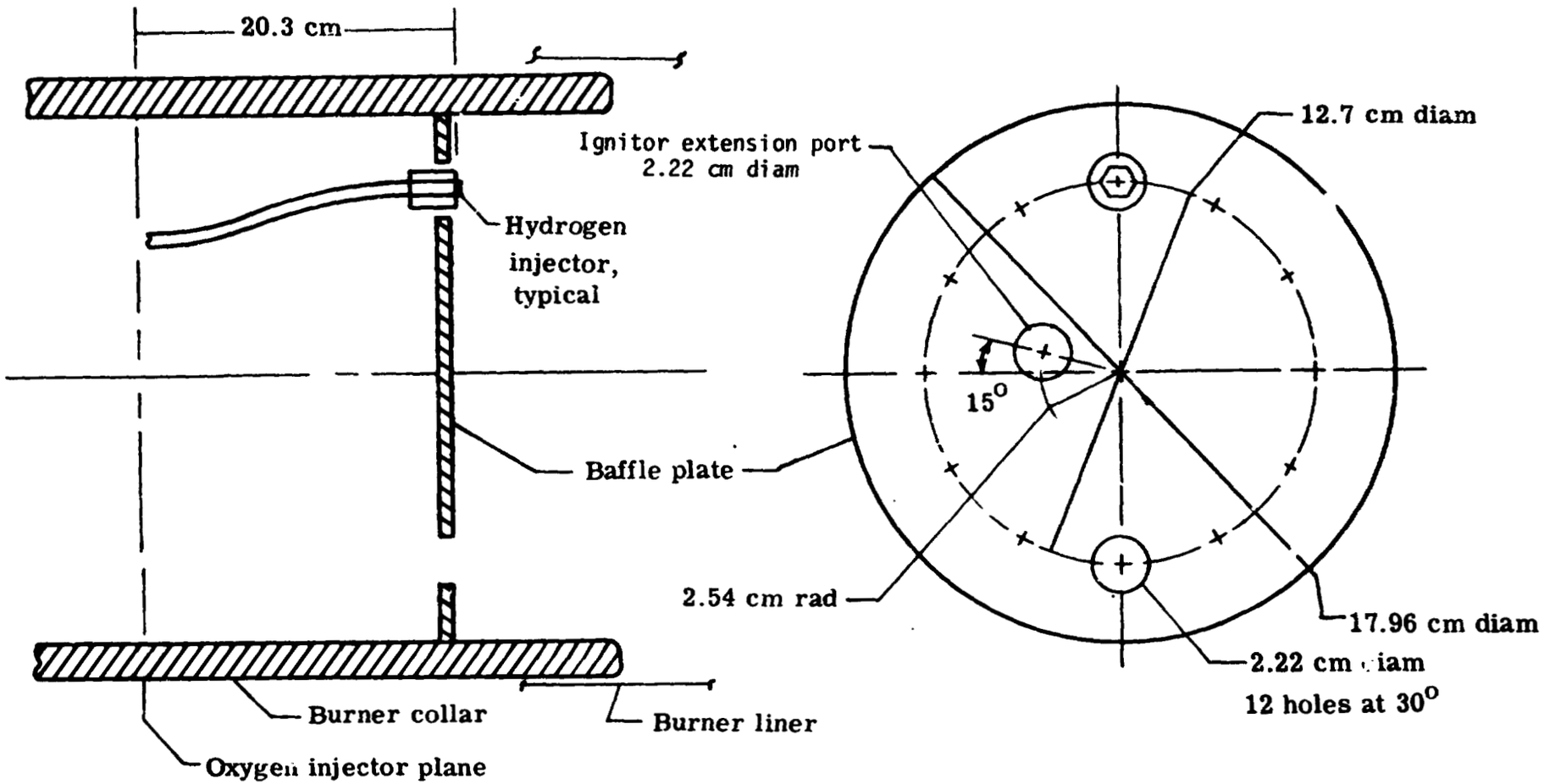


(a) Hydrogen injector configuration

Figure 6.- Burner injector configuration, hydrogen injectors off-set and extended with baffle and reduced survey data.

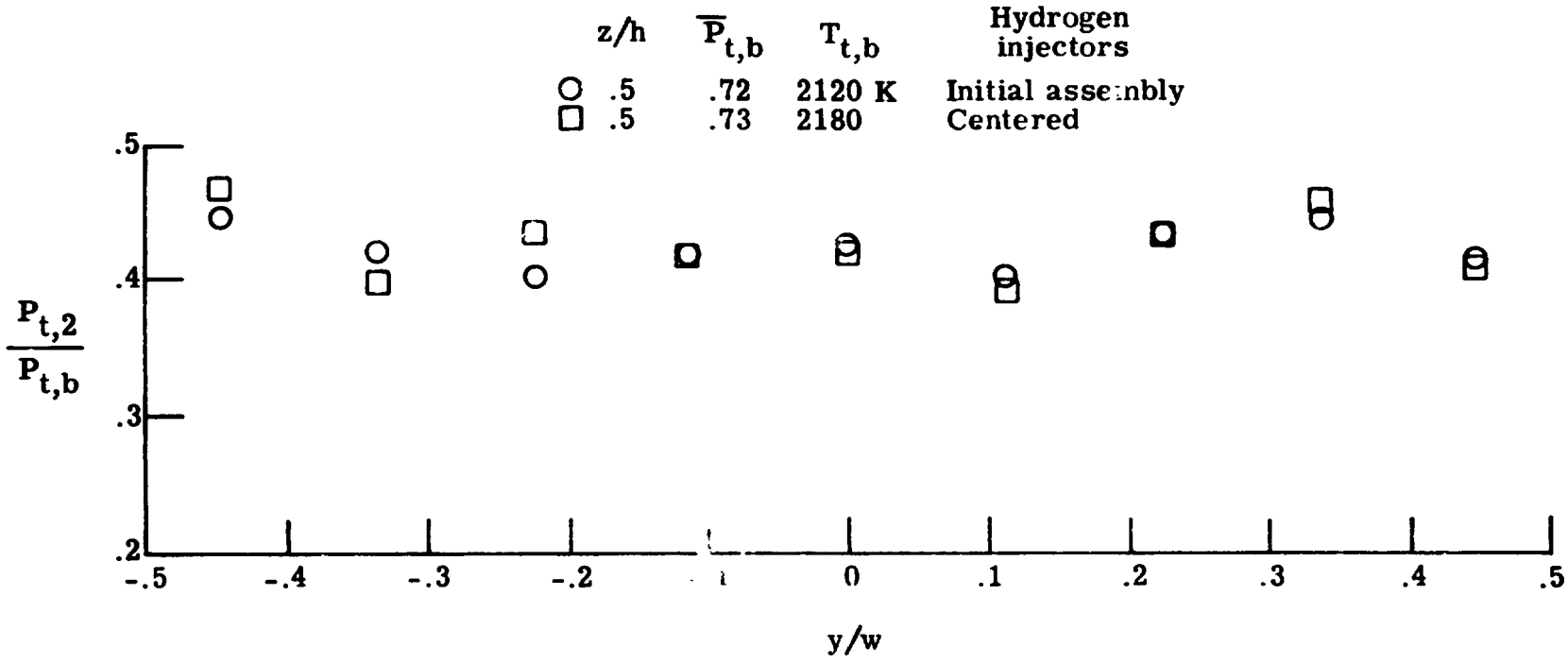


(b) Nondimensional pitot pressure distribution

Figure 6.- Continued

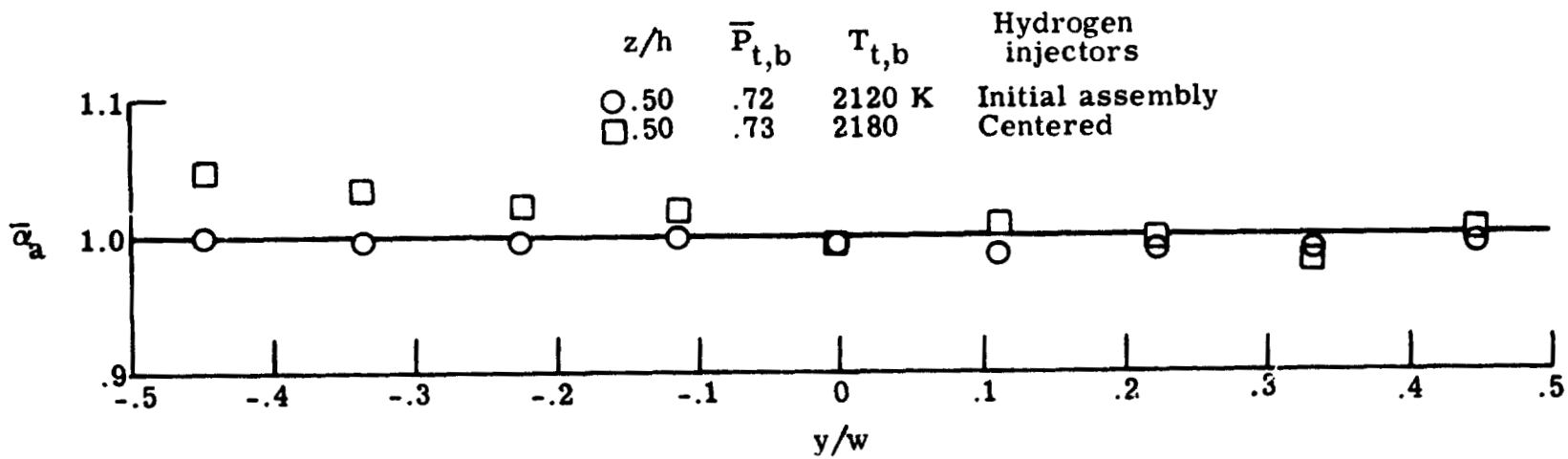


(c) Local to bulk air distribution ratio

Figure 6.- Continued

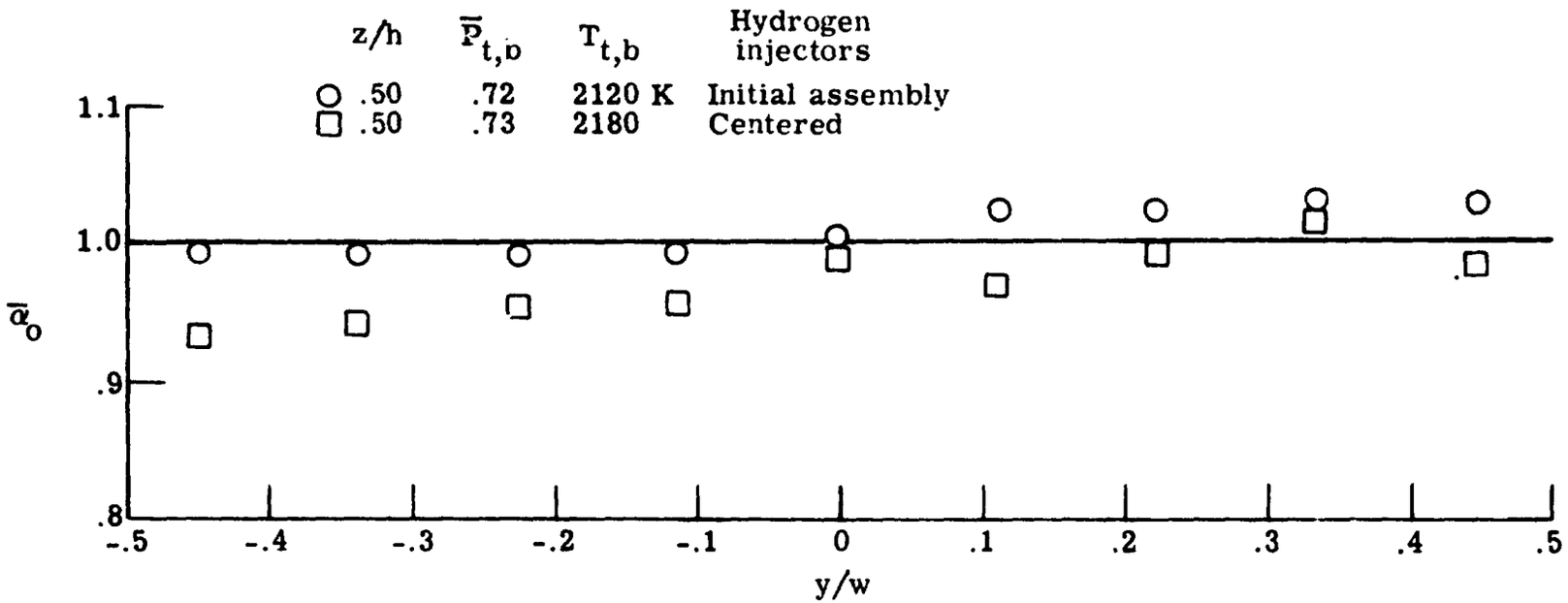


(d) Local to bulk oxygen distribution ratio

Figure 6.- Continued

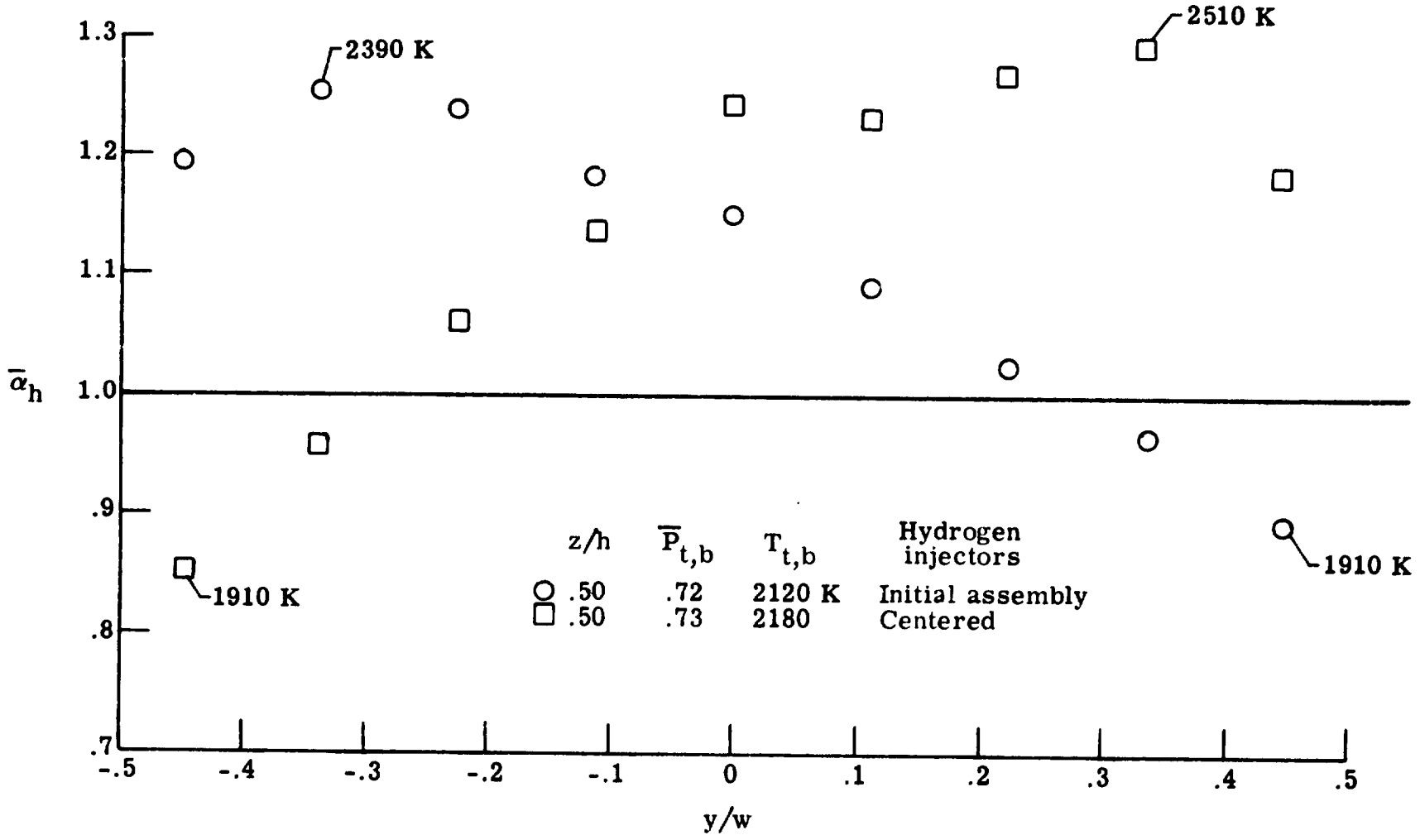


(e) Local to bulk hydrogen distribution ratio

Figure 6.- Concluded

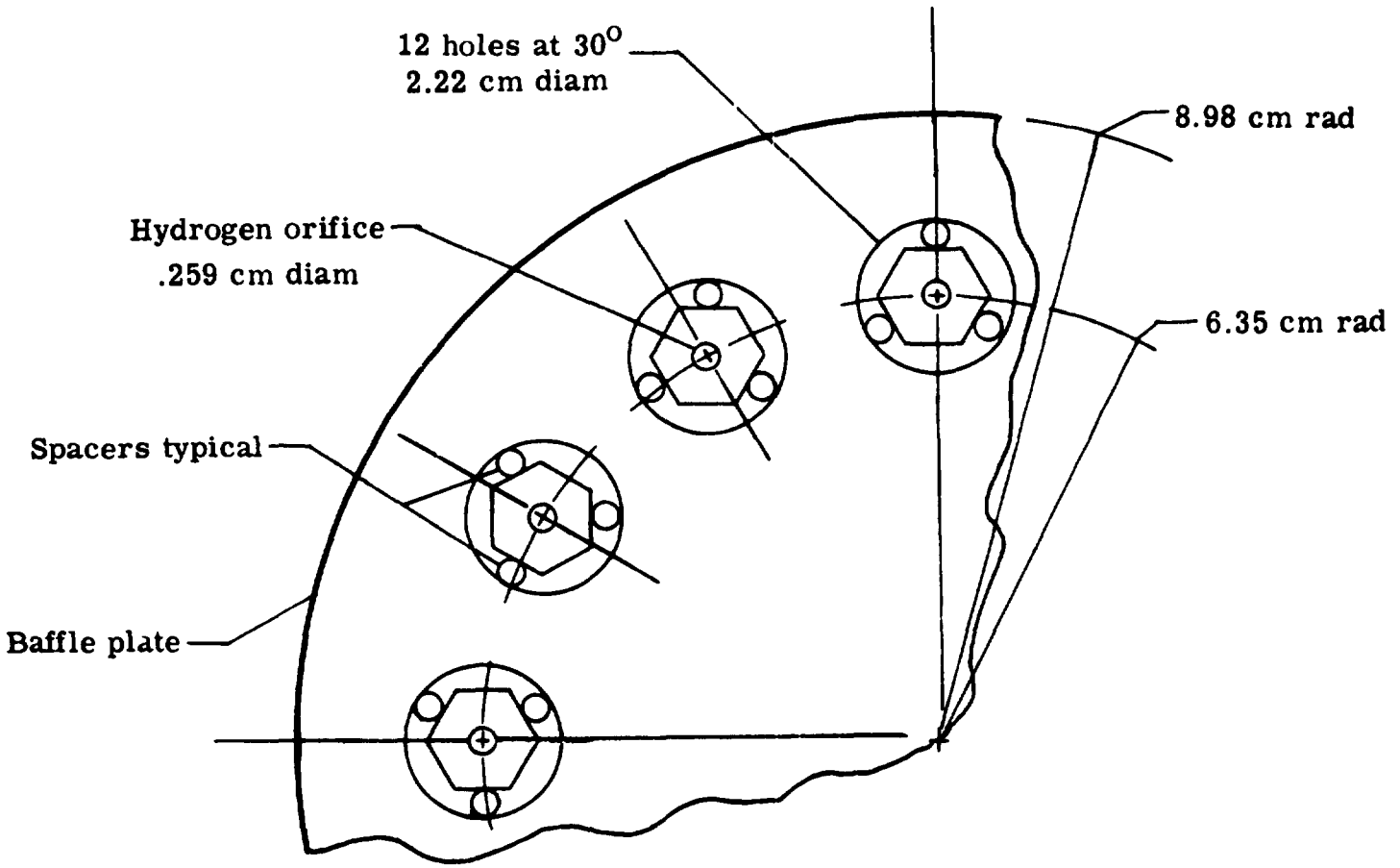


(a) Self-centering injector configuration

Figure 7.- Burner self-centering injector configuration and reduced survey data.

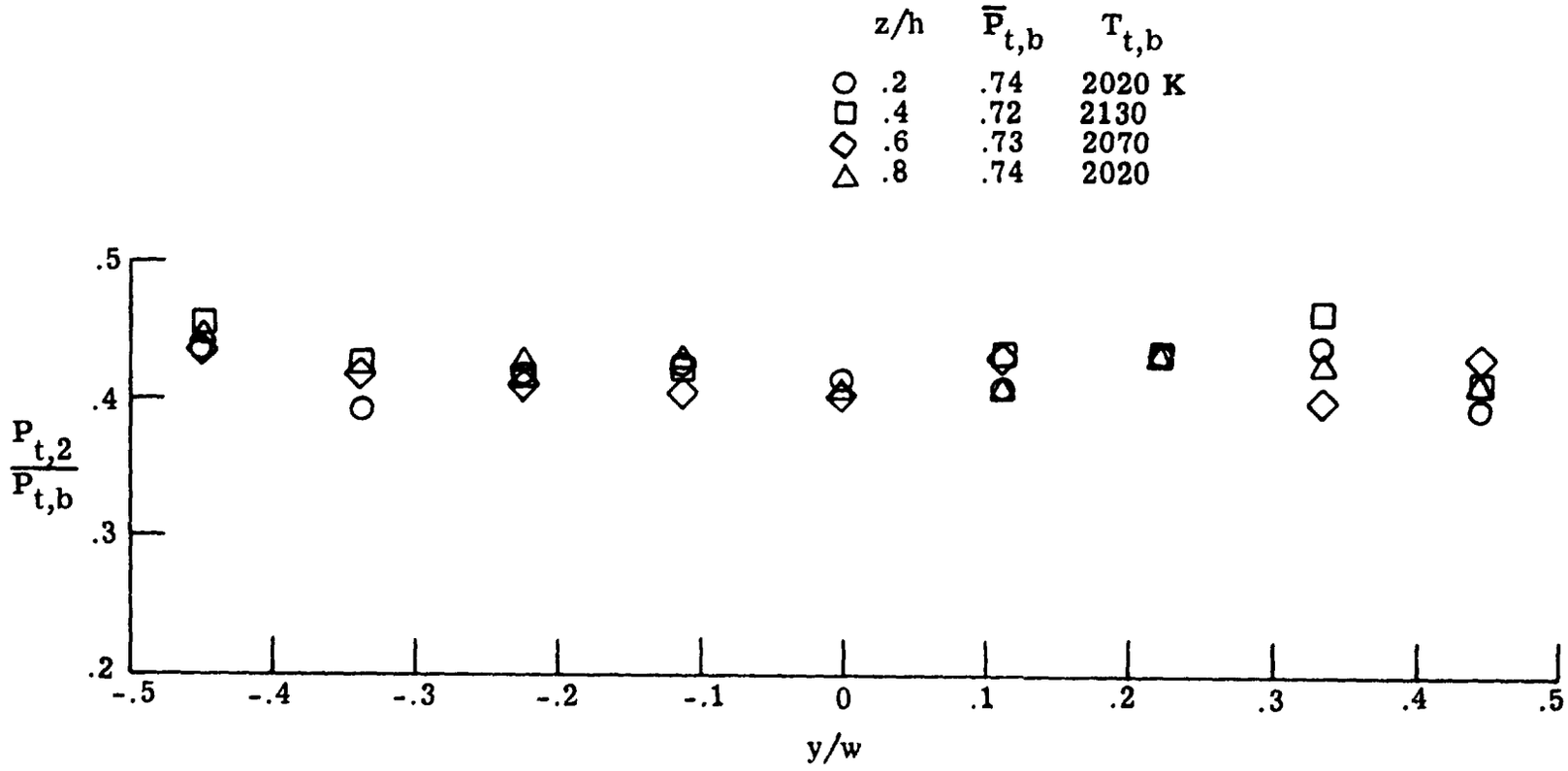


(b) Nondimensional pitot pressure distribution

Figure 7.- Continued

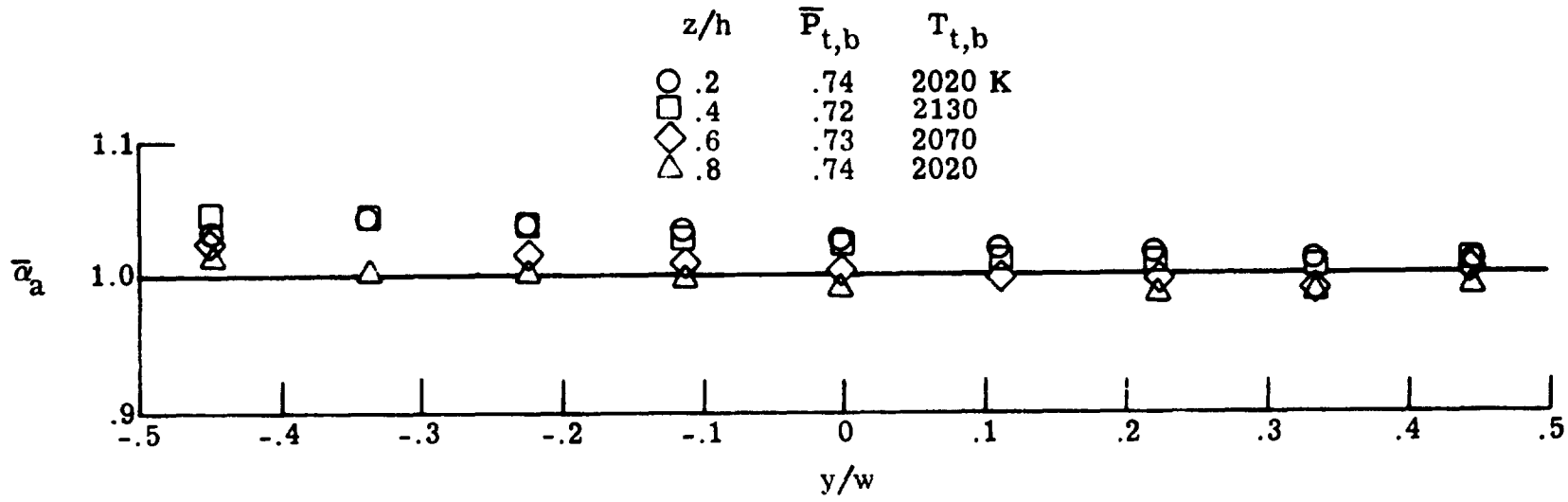


(c) Local to bulk air distribution ratio

Figure 7.- Continued

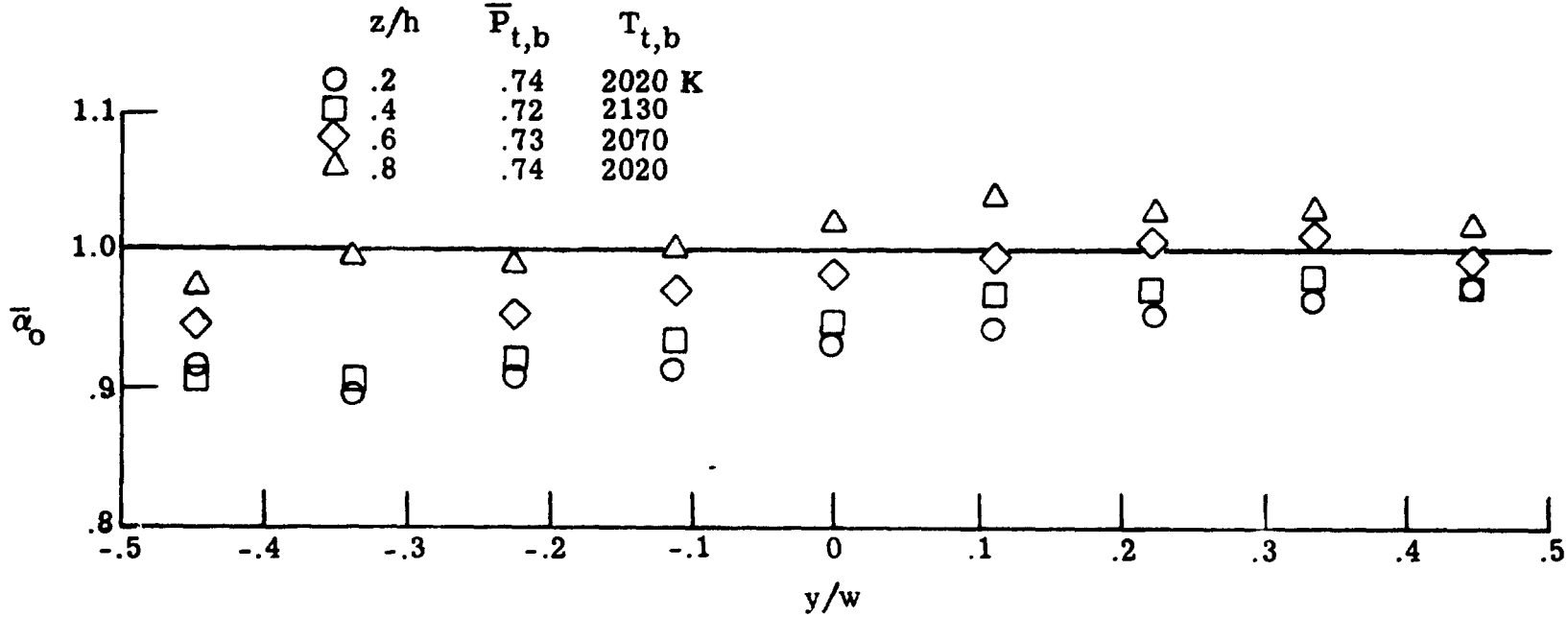


(d) Local to bulk oxygen distribution

Figure 7.- Continued

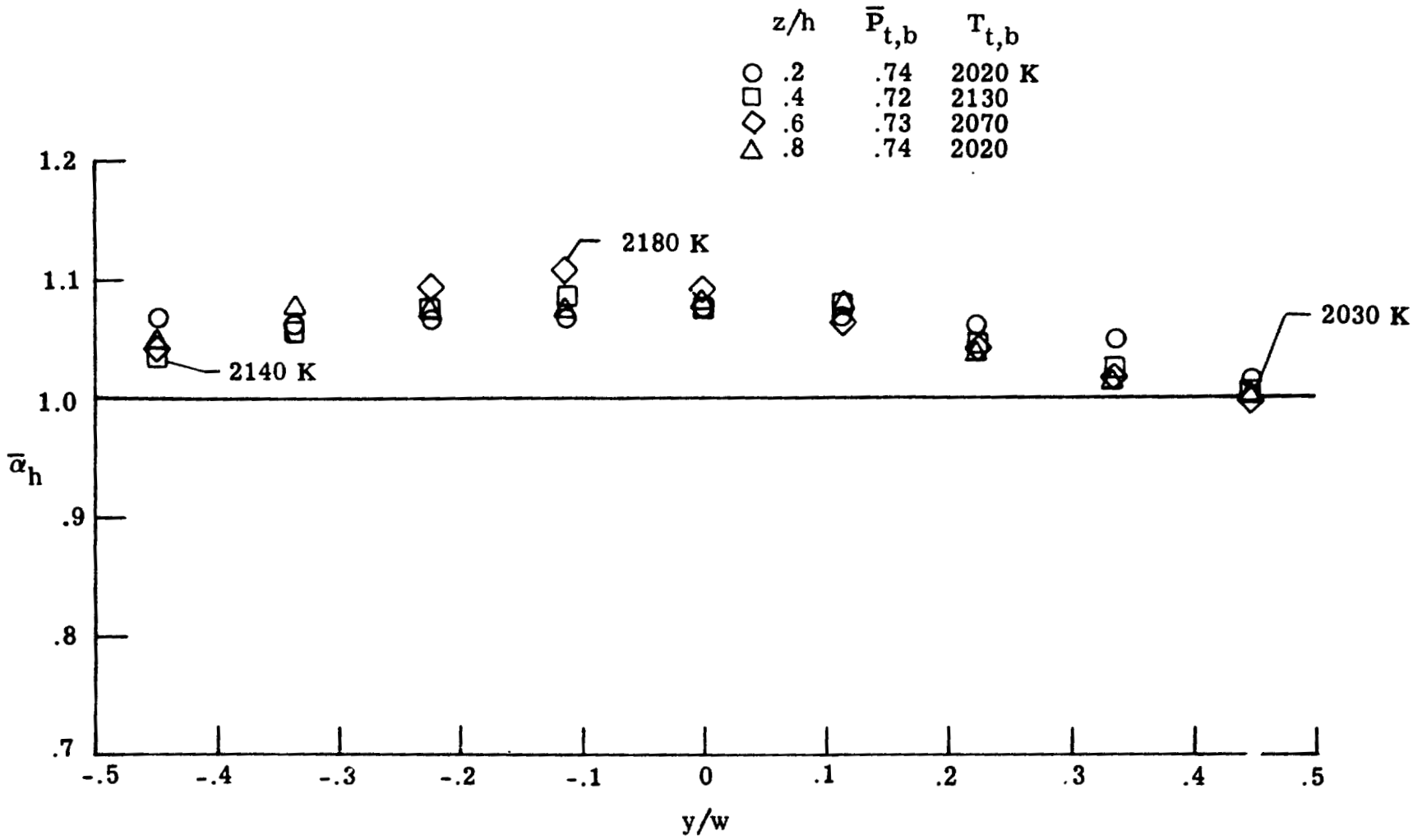


(e) Local to bulk hydrogen distribution ratio

Figure 7.- Concluded